Supporting Information

Cyclometalated *Z*-Selective Ruthenium Metathesis Catalysts with Modified *N*-Chelating Groups

Myles B. Herbert,[†,§] Benjamin A. Suslick,[†,§] Peng Liu,[‡] Lufeng Zou,[‡] Peter K. Dornan,[†] K.N. Houk,[‡,*] R. H. Grubbs[†,*]

† Arnold and Mabel Beckman Laboratory of Chemical Synthesis, Division of Chemistry and Chemical Engineering, California Institute of Technology, Pasadena, California 91125, United States

‡ Department of Chemistry and Biochemistry, University of California, Los Angeles, 90095-1569, United States.

Table of Contents

List of Figures

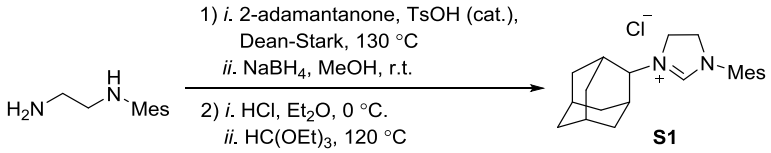

Synthesis of S1.

N-mesitylethylenediamine[1] (1.82 g, 10.2 mmol) and 2-adamantanone (1.53 g, 10.2 mmol) were taken up in toluene (100 mL). *p*-Toluenesulfonic acid monohydrate (20 mg, 0.1 mmol) was added and the mixture was headed to 130 °C overnight using a Dean-Stark apparatus. Upon cooling to room temperature, the solvent was removed *in vacuo*. The crude mixture was taken up in MeOH (100 mL) and $NaBH_4$ (1.58 g, 41.8 mmol) was slowly added as a solid. After stirring at room temperature for 2 hours, the solvent was removed *in vacuo* and the crude mixture was taken up in Et_2O (50 mL). The mixture was then washed with water (3 x 25 mL) and brine (1 x 50 mL), and dried over Na_2SO_4. The Et_2O mixture was used without further purification and treated with a solution of HCl in 1,4-dioxane (4M, 5.1 mL) causing precipitation of a white solid. This was isolated and added to a flask containing trimethylorthoformate (20 mL). The reaction was stirred for 120 °C for 2 hours. After warming to room temperature, Et_2O was added, causing precipitation of the pure desired product as a white solid (2.0 g, 5.6 mmol, 55%). ^{1}H NMR (500 MHz, $CDCl_3$): δ 8.56 (s, 1H), 6.90 (s, 2H), 4.33-4.05 (m, 4H), 4.05 (s, 1H), 2.45 (s, 2H), 2.34 (s, 6H), 2.25 (s, 3H), 2.19 (s, 1H), 1.92-1.86 (m, 6H), 1.75 (s, 2H), 1.71 (s, 3H). ^{13}C{^{1}H} NMR (125 MHz,$CDCl_3$):δ 158.3, 140.3, 135.6, 131.1, 130.1, 62.9, 50.9, 48.3, 37.1, 36.4, 31.4, 29.9, 27.1, 21.1, 18.3; HRMS-FAB (*m/z*) $[M]^+$ calcd for $C_{22}H_{31}N_2$, 323.2487; found, 323.2475.

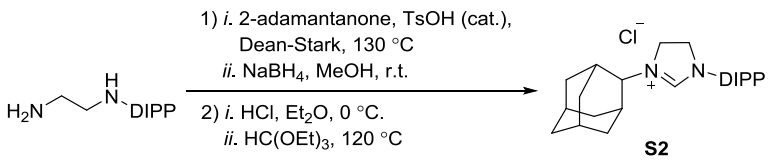

Synthesis of S2.

N-2,6-diisopropylphenylethylenediamine[1] (865 mg, 3.93 mmol) and 2-adamantanone (592 g, 3.93 mmol) were taken up in toluene (40 mL). *p*-Toluenesulfonic acid monohydrate (8 mg, 0.04 mmol) was added and the mixture was headed to 130 ˚C overnight using a Dean-Stark apparatus. Upon cooling to room temperature, the solvent was removed *in vacuo*. The crude mixture was taken up in MeOH (50 mL) and $NaBH_4$ (608 mg, 16.1 mmol) was slowly added as a solid. After stirring at room temperature for 2 hours, the solvent was removed *in vacuo* and the crude mixture was taken up in Et_2O (30 mL). The mixture was then washed with water (3 x 15 mL) and brine (1 x 25 mL), and dried over Na_2SO_4. The Et_2O mixture was used without further purification and treated with a solution of HCl in Et_2O (1M, 8.24 mL) causing precipitation of a white solid. This was isolated and added to a flask containing trimethylorthoformate (8 mL). The reaction was stirred for 120 ˚C for 2 hours. After warming to room temperature, Et_2O was added, causing precipitation of the pure desired product as a white solid (843 mg, 2.1 mmol, 54% overall yield). ^{1}H NMR (500 MHz, $CDCl_3$): δ 8.29 (s, 1H), 7.41 (t, *J* = 7.74, 1H), 7.23 (d, *J* = 7.77, 2H), 4.47 (t, *J* = 9.69, 2H), 4.29 (t, *J* = 9.38, 2H), 4.18 (s, 1H), 2.44 (s, 2H), 1.93 (s, 6H), 1.77-1.71 (m, 6H), 1.28 (t, *J* = 6.13, 12H); ^{13}C{^{1}H} NMR (125 MHz, $CDCl_3$): δ 157.6, 147.1, 131.2, 130.5, 125.1, 62.8, 53.6, 48.6, 37.0, 36.4, 31.5, 29.9, 28.9, 27.1, 26.9, 25.2, 24.6; HRMS-FAB (*m/z*) $[M]^+$ calcd for $C_{25}H_{37}N_2$, 365.2957; found, 365.2971.

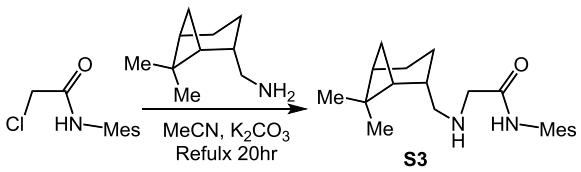

S3

Synthesis of S3.

To a flame dried 2-neck flask under argon was added 2-chloro-N-mesitylacetamide (1.34 g, 6.34 mmol, 1.2 eq), K_2CO_3 (1.69 g, 12.6 mmol, 2.4 eq), acetonitrile (35 mL) and then (-)-cis-myrtanylamine (0.874 mL, 5.22 mmol, 1.0 eq). A condenser was attached, and the reaction mixture was heated to reflux for 20 hr. The crude mixture was cooled to ambient temperature, filtered over Celite, washed with CH_2Cl_2, and concentrated *in vacuo*. The title compound was purified by column chromatography (7:3 ethyl acetate : hexanes) to give a clear viscous oil (1.33 g, 78%). ^{1}H NMR (500 MHz, $CDCl_3$): δ 8.75 (s, 1H), 6.90 (s, 2H), 3.45 (d, J = 17.1 Hz, 1H), 3.40 (d, *J* = 17.1 Hz, 1H), 2.75 (dd, *J* = 11.5, 7.0 Hz, 1H), 2.71 (dd, *J* = 11.4, 7.9 Hz, 1H), 2.38 (dtd, *J* = 9.5, 6.3, 2.0 Hz, 1H), 2.27 (s, 3H), 2.23-2.16 (m, 1H), 2.19 (s, 6H), 2.03-

1.84 (m, 5H), 1.55-1.47 (m, 1H), 1.18 (s, 3H), 0.99 (s, 3H), 0.93 (d, *J* = 9.6 Hz, 1H); $^{13}C\{^{1}H\}$ NMR (126 MHz, $CDCl_3$): δ 170.6, 136.8, 134.9, 131.3, 129.0, 57.2, 52.9, 44.6, 42.2, 41.6, 38.8, 33.6, 28.2, 26.2, 23.5, 21.0, 20.8, 18.6; HRMS-FAB (*m/z*) $[M + H]^+$ calcd for $C_{21}H_{34}ON_2$, 329.2593; found, 329.2589.

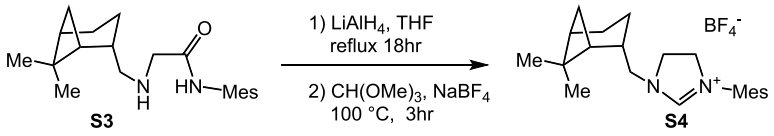

Synthesis of S4.

To a flame dried 2-neck flask under argon was added $LiAlH_4$ (463 mg, 12.2 mmol, 3.9 eq) and THF (20 mL). Amide **S3** (1.03 g, 3.14 mmol, 1 eq) was then added as a solution in THF (5 mL). A condenser was added and the reaction mixture was heated to reflux for 18 hr. The crude mixture was cooled to ambient temperature and quenched by dropwise addition of H_2O (5 mL) and then NaOH (1 mL) followed by brine (5 mL). The mixture was extracted with ethyl acetate (20 mL) and then CH_2Cl_2 (2 x 15 mL). The combined organics were dried with $MgSO_4$ and concentrated *in vacuo* to yield a yellow oil (965 mg) which was used without further purification. The oil was dissolved in $CH(OMe)_3$ (6.5 mL) and NH_4BF_4 (341 mg, 3.25 mmol) was then added. A reflux condenser was added and the reaction mixture was heated to 100 °C for 3 hr. The crude mixture was cooled to ambient temperature and concentrated *in vacuo* to give an wet red solid. The solid was then triterated with hexanes, followed by ether, followed by 1:1 ether : ethyl acetate to give a tan powder (622 mg, 51%). ^{1}H NMR (500 MHz, $CDCl_3$): δ 7.93 (d, *J* = 4.5 Hz, 1H), 6.91 (s, 2H), 4.24-4.11 (m, 4H), 3.74-3.58 (m, 2H), 2.52-2.38 (m, 2H), 2.28 (s, 3H), 2.25 (s, 3H), 2.25 (s, 3H), 2.03-1.83 (m, 5H), 1.53-1.42 (m, 1H), 1.19 (s, 3H), 1.02 (s, 3H), 0.98 (d, *J* = 9.6 Hz, 1H); $^{13}C\{^{1}H\}$ NMR (126 MHz, $CDCl_3$): δ 158.1, 140.3, 135.6, 130.6, 130.0, 54.2, 51.0, 48.9, 43.6, 41.2, 38.7, 38.3, 33.2, 27.9, 25.8, 23.3, 21.2, 19.4, 17.6; HRMS-FAB (*m/z*) $[M]^+$ calcd for $C_{22}H_{33}N_2$, 325.2644; found, 325.2642.

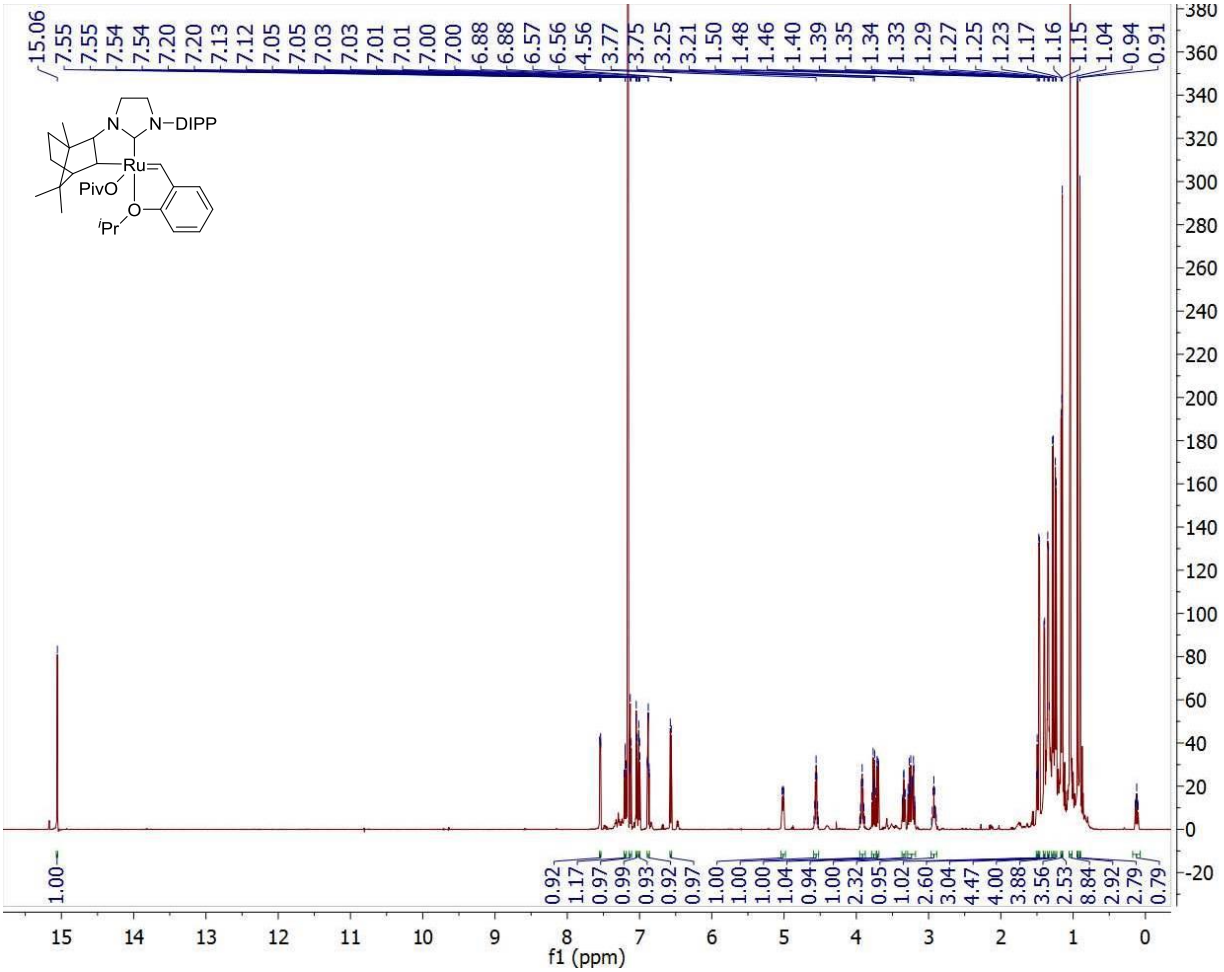

Figure S1. ^{1}H NMR (600 MHz) spectrum of **11** in C_6D_6.

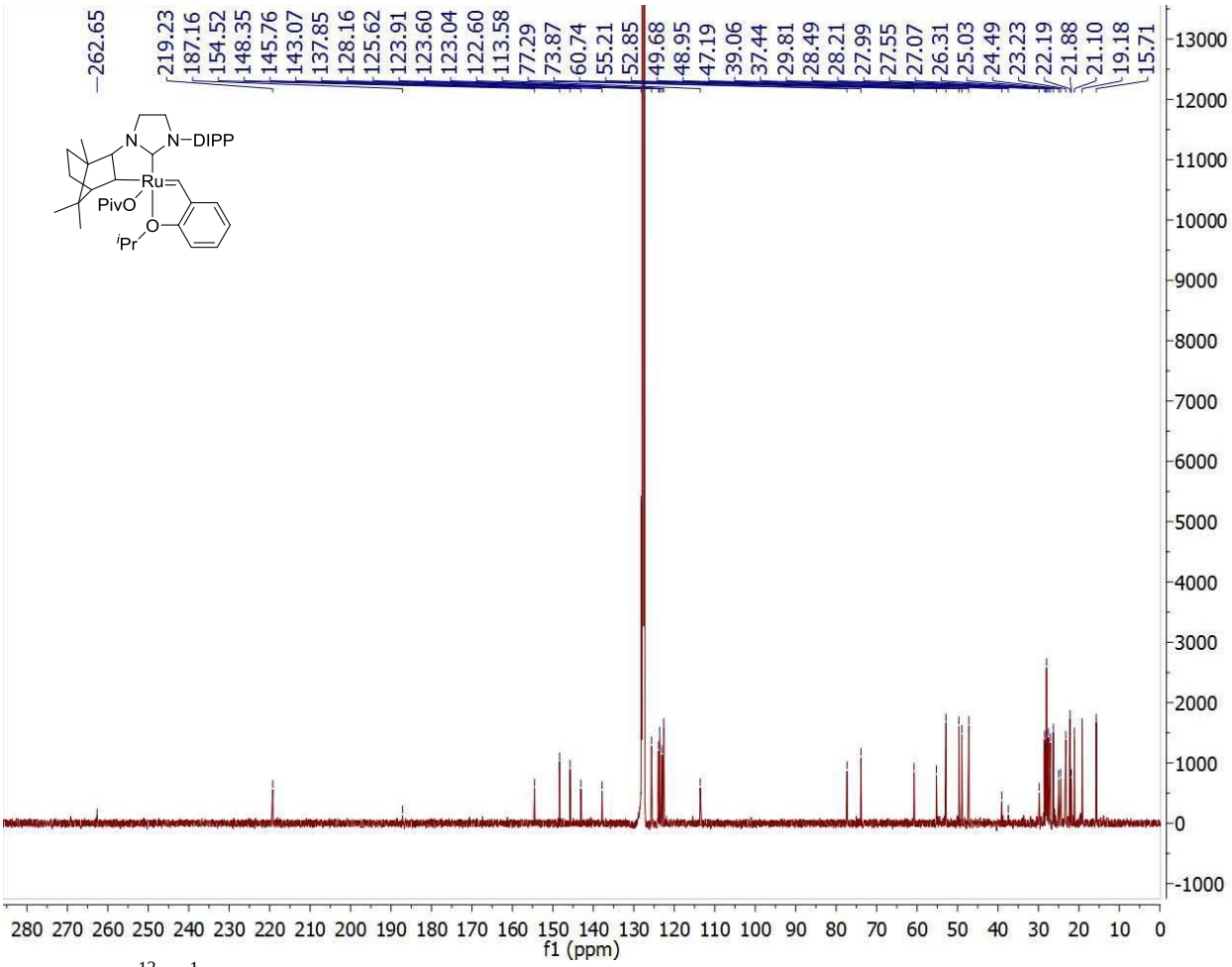

Figure S2. $^{13}C\{^{1}H\}$ NMR (126 MHz) spectrum of **11** in C_6D_6.

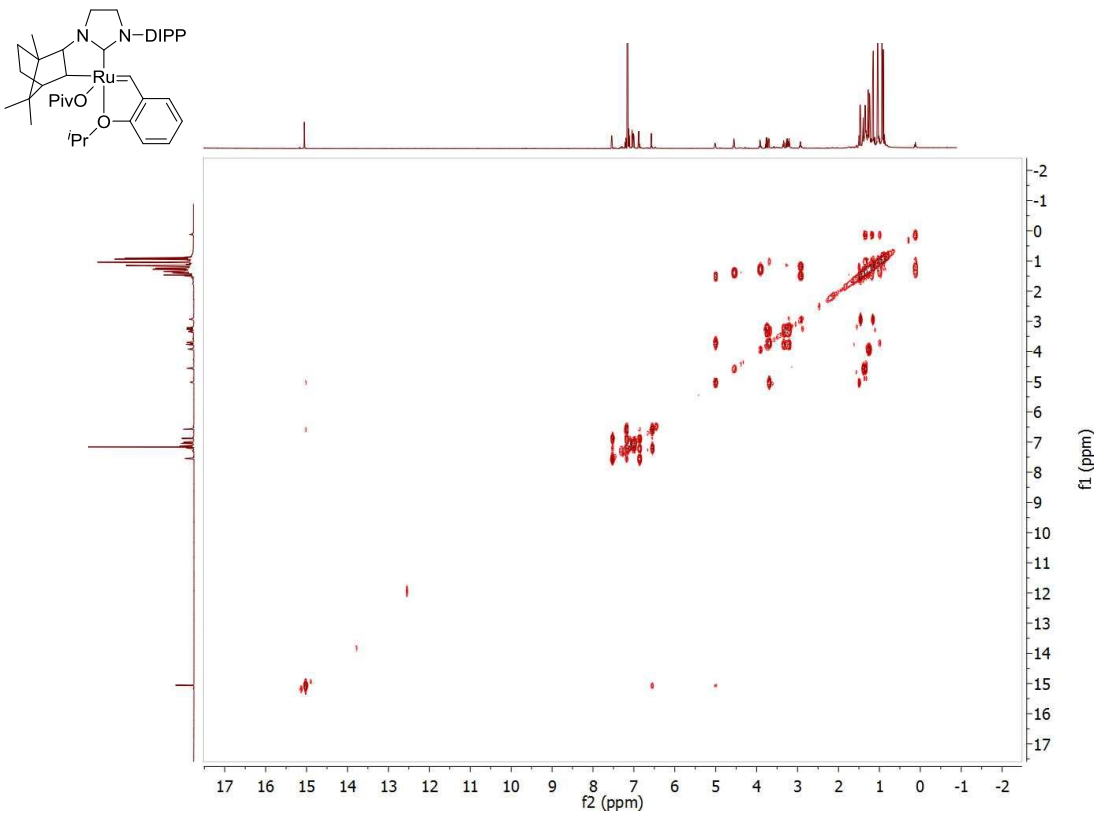

Figure S3. ^{1}H-^{1}H Coupled gCOSY spectrum of **11** in C_6D_6.

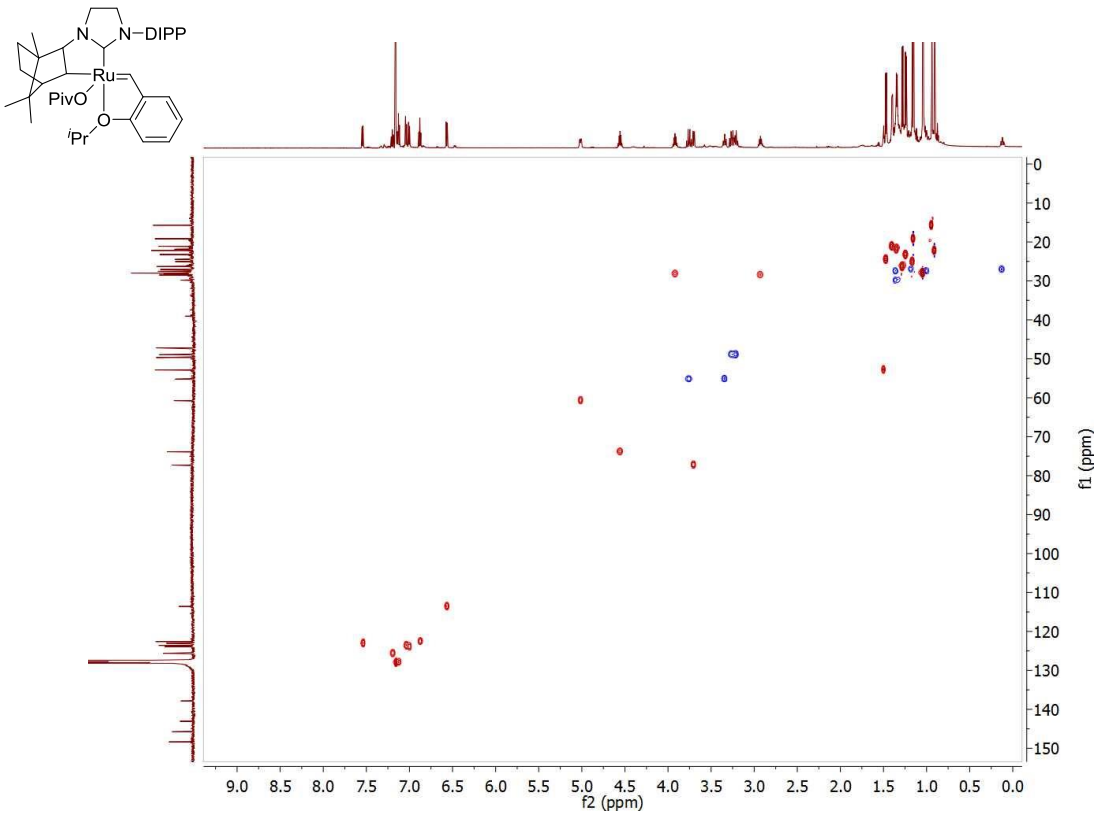

Figure S4. ^{1}H-^{13}C Coupled gHSQC spectrum of **11** in C_6D_6.

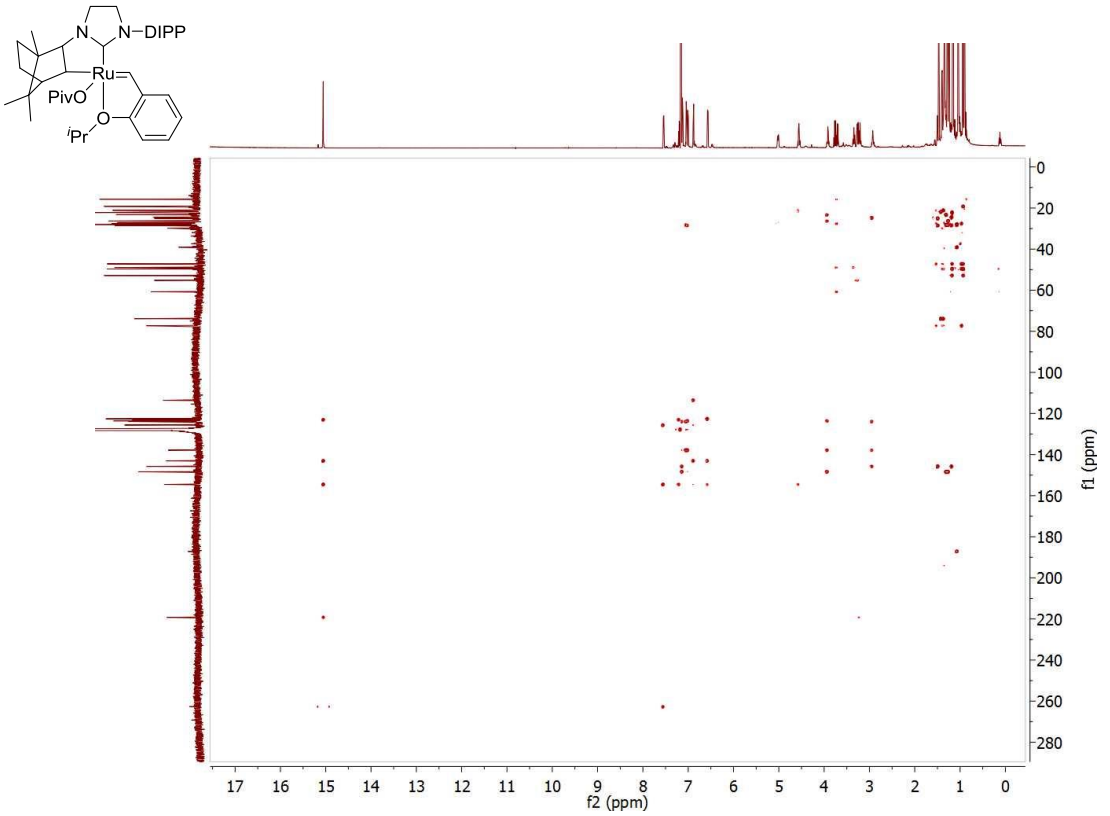

Figure S5. ^{1}H-^{13}C Coupled gHMBC spectrum of **11** in C_6D_6.

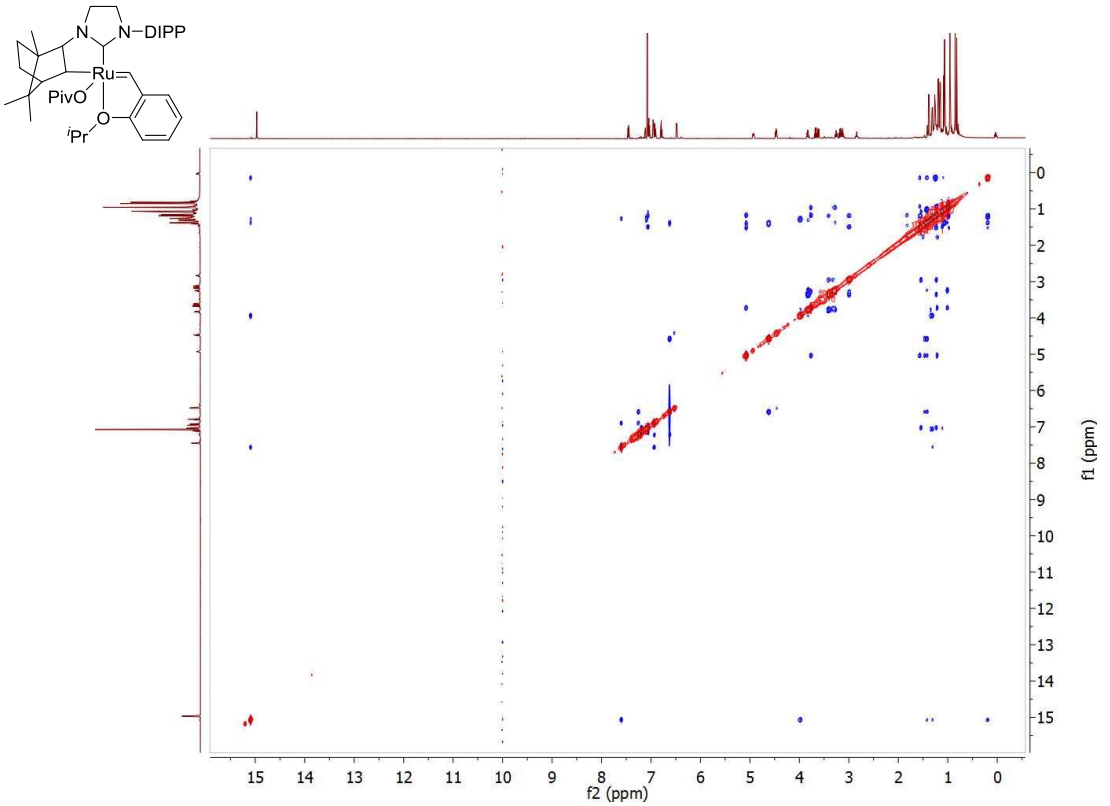

Figure S6. ^{1}H-^{1}H Coupled NOESY spectrum of **11** in C_6D_6.

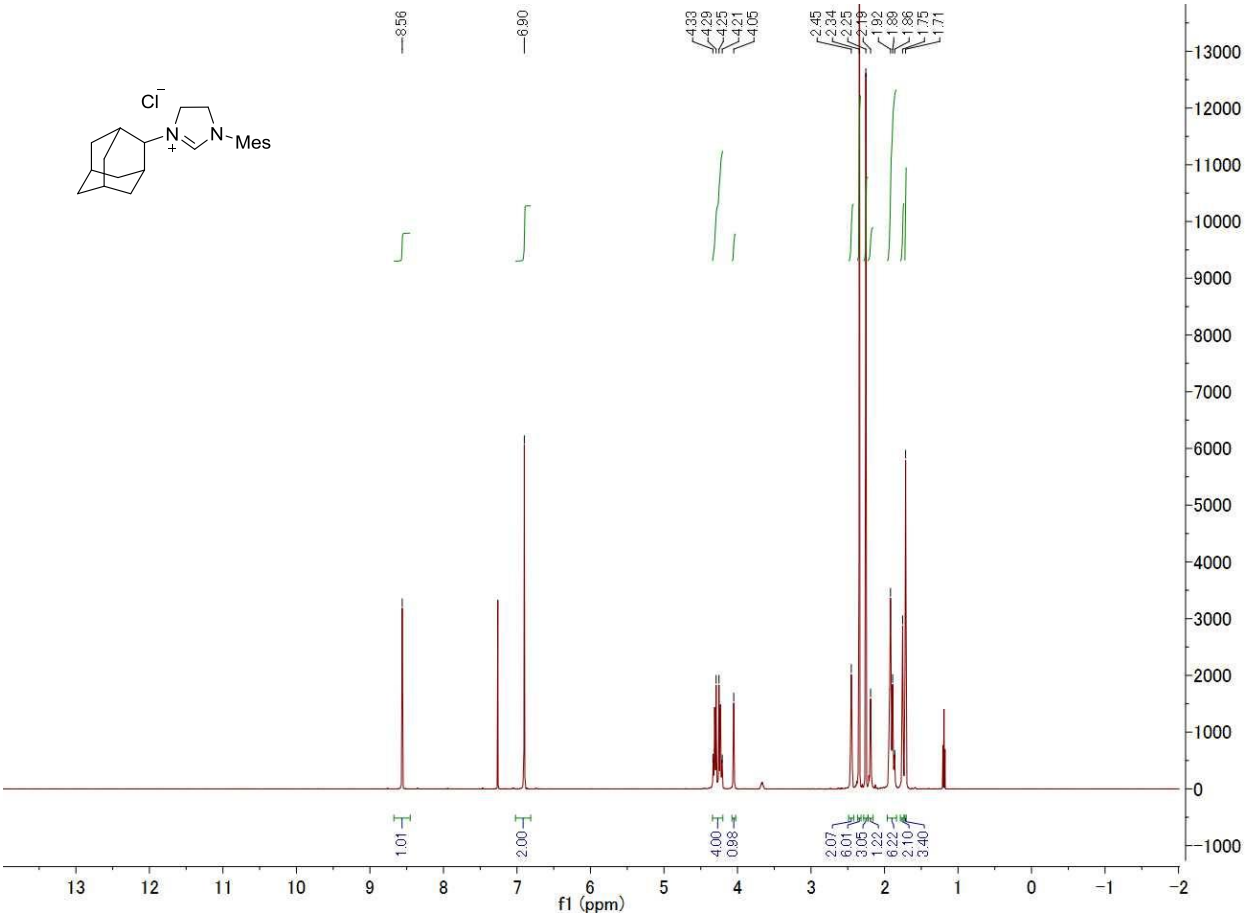

Figure S7. ^{1}H NMR (500 MHz) spectrum of **S1** in $CDCl_3$.

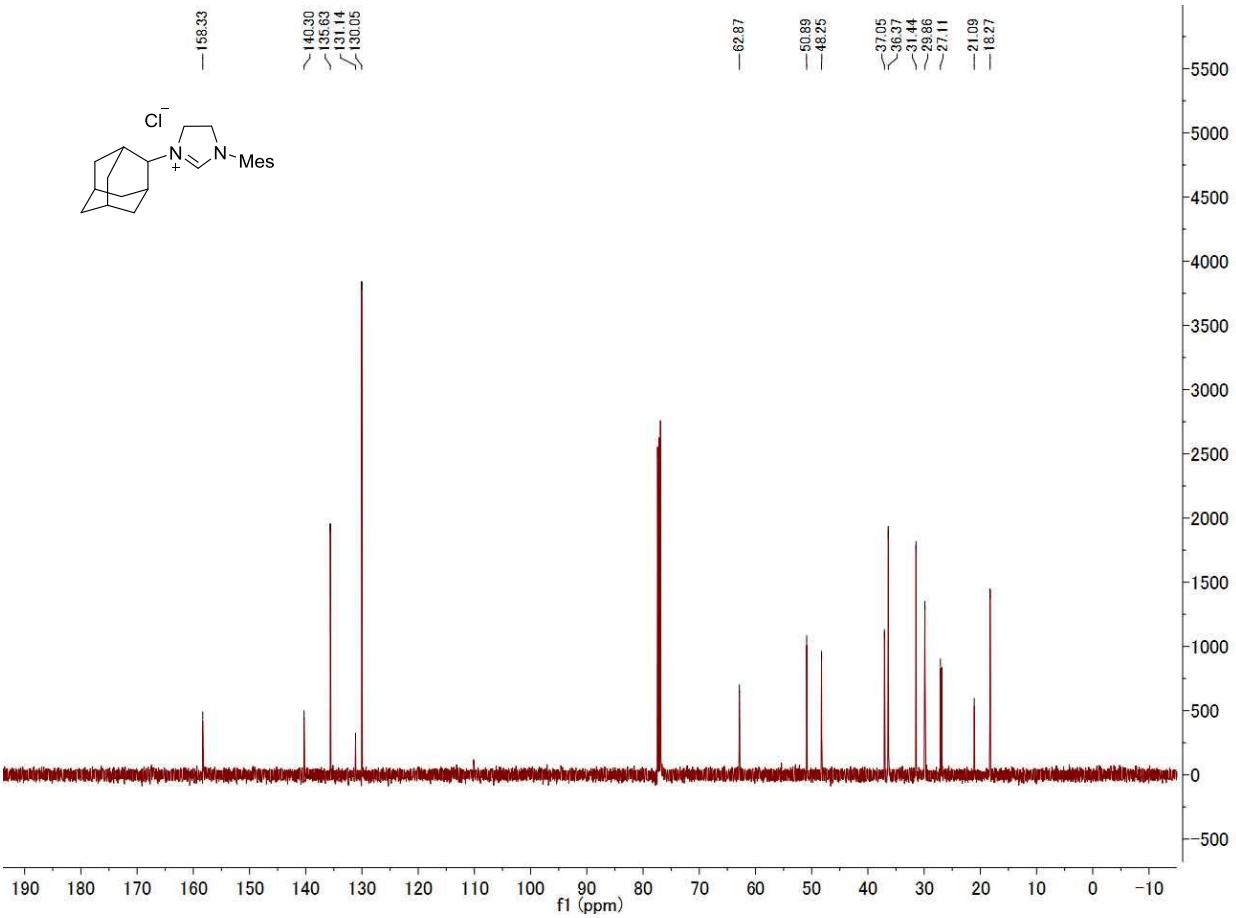

Figure S8. $^{13}C\{^{1}H\}$ NMR (125 MHz) spectrum of **S1** in $CDCl_3$.

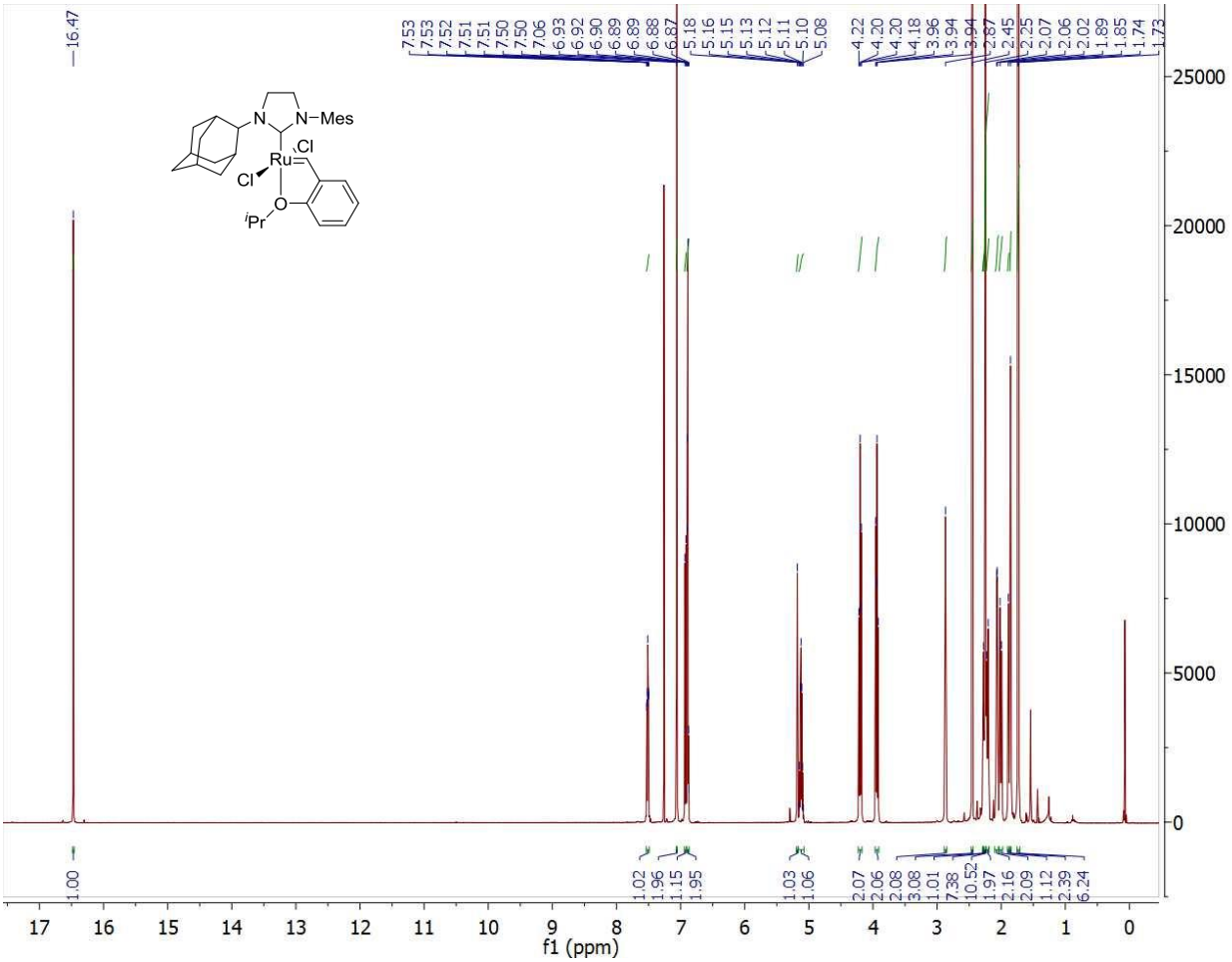

Figure S9. ^{1}H NMR (500 MHz) spectrum of **15** in $CDCl_3$.

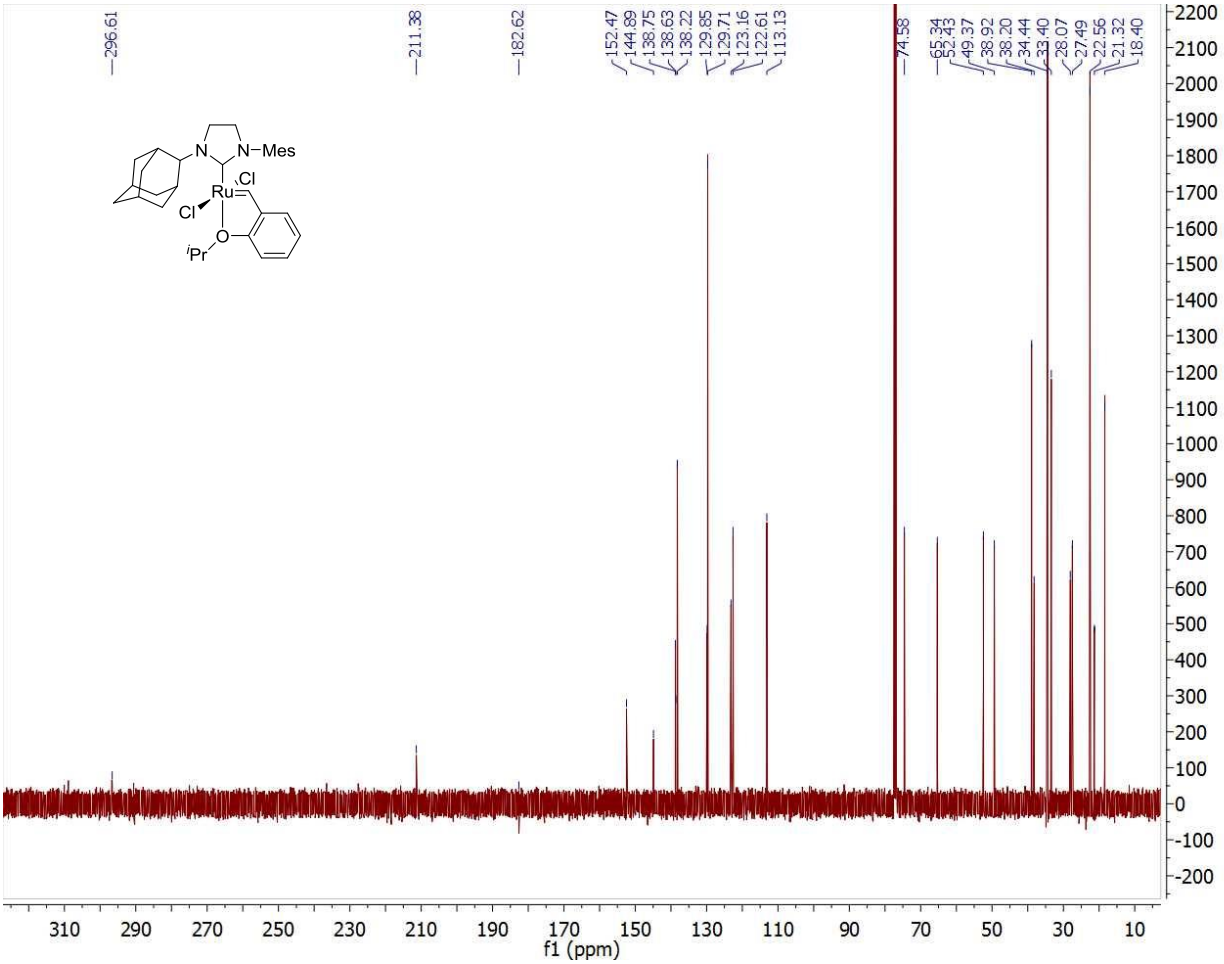

Figure S10. $^{13}C\{^{1}H\}$ NMR (126 MHz) spectrum of **15** in $CDCl_3$.

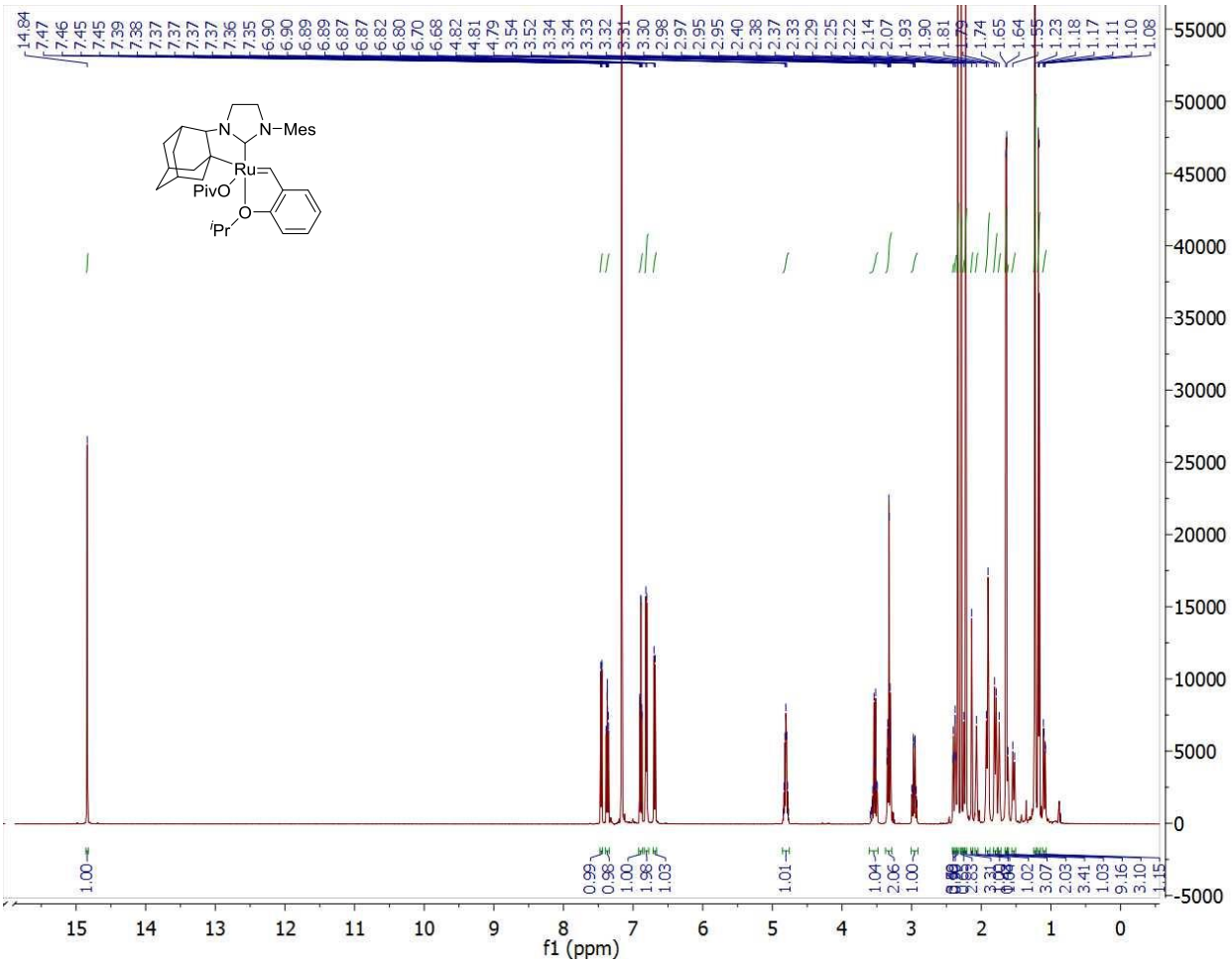

Figure S11. ^{1}H NMR (500 MHz) spectrum of **16** in C_6D_6.

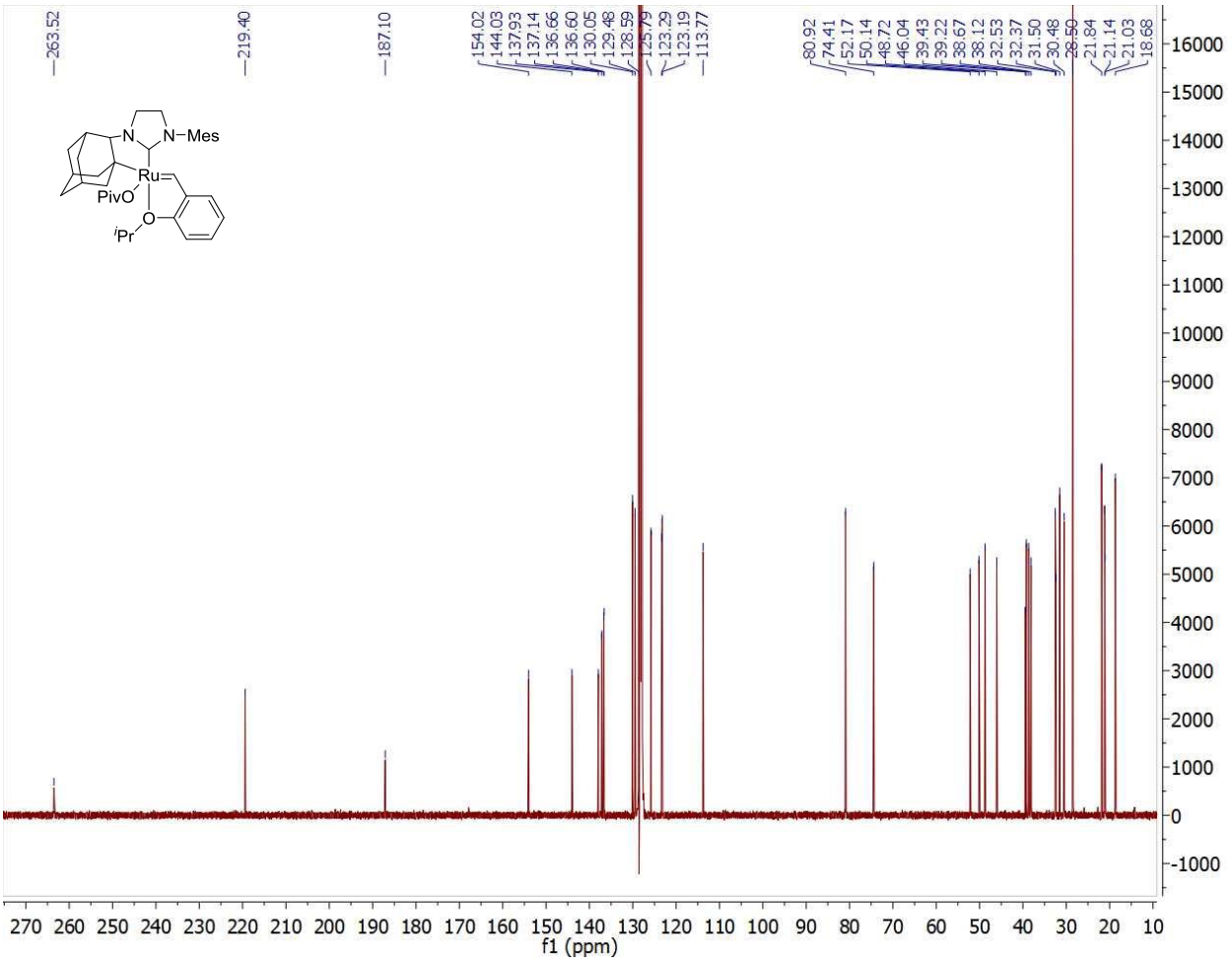

Figure S12. $^{13}C\{^{1}H\}$ NMR (126 MHz) spectrum of **16** in C_6D_6.

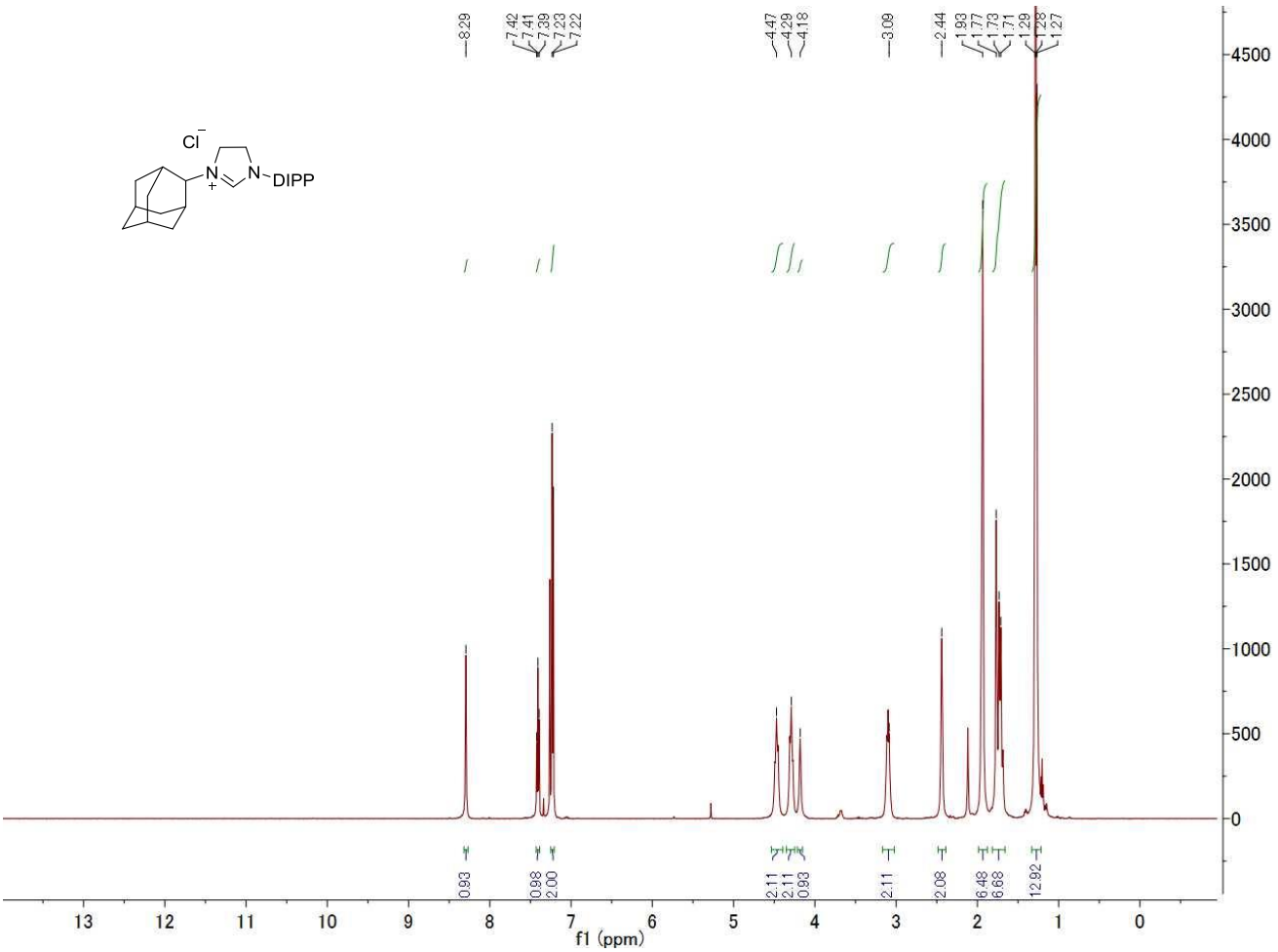

Figure S13. ^{1}H NMR (500 MHz) spectrum of **S2** in $CDCl_3$.

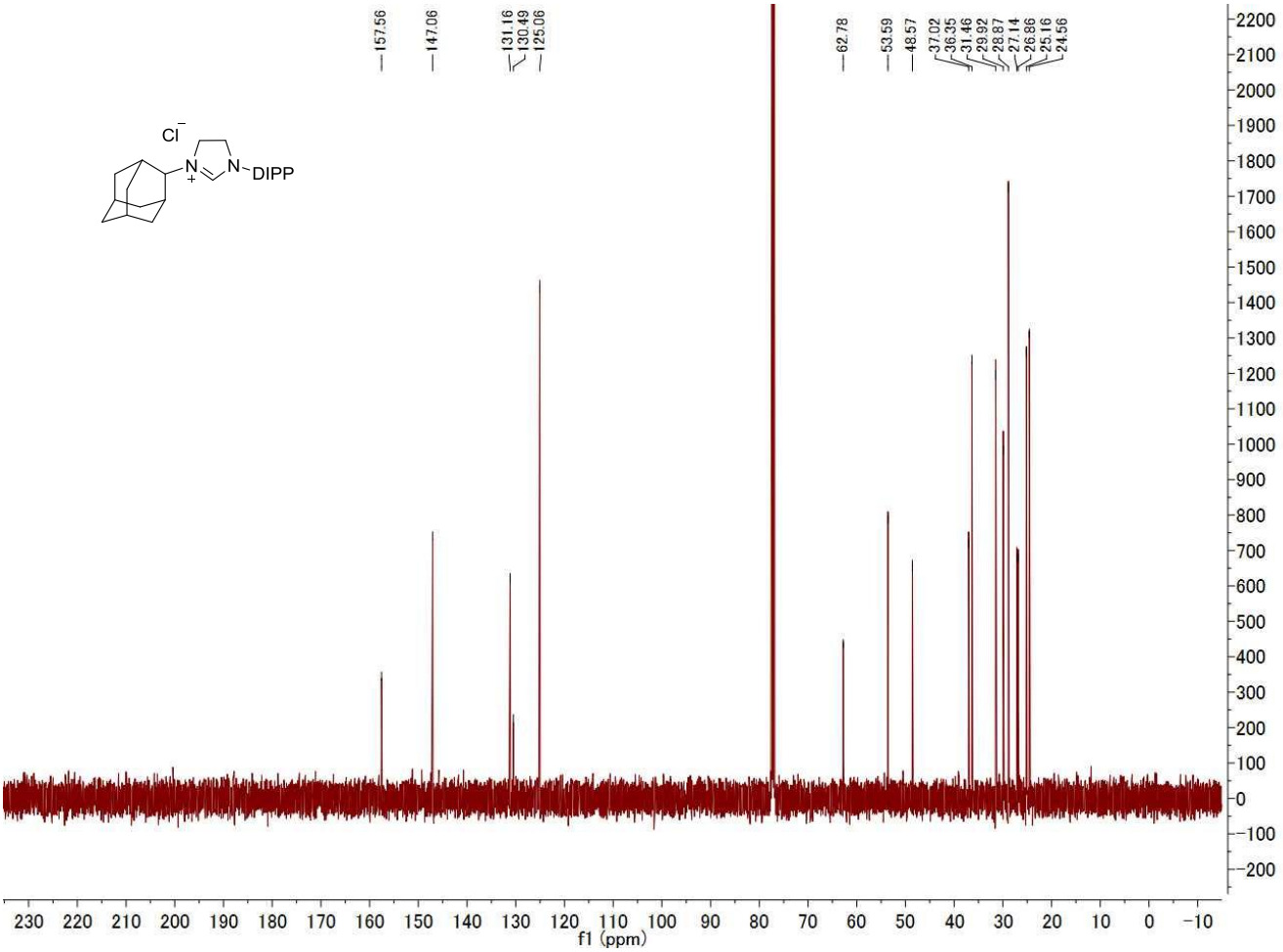

Figure S14. $^{13}C\{^{1}H\}$ NMR (125 MHz) spectrum of **S2** in $CDCl_3$.

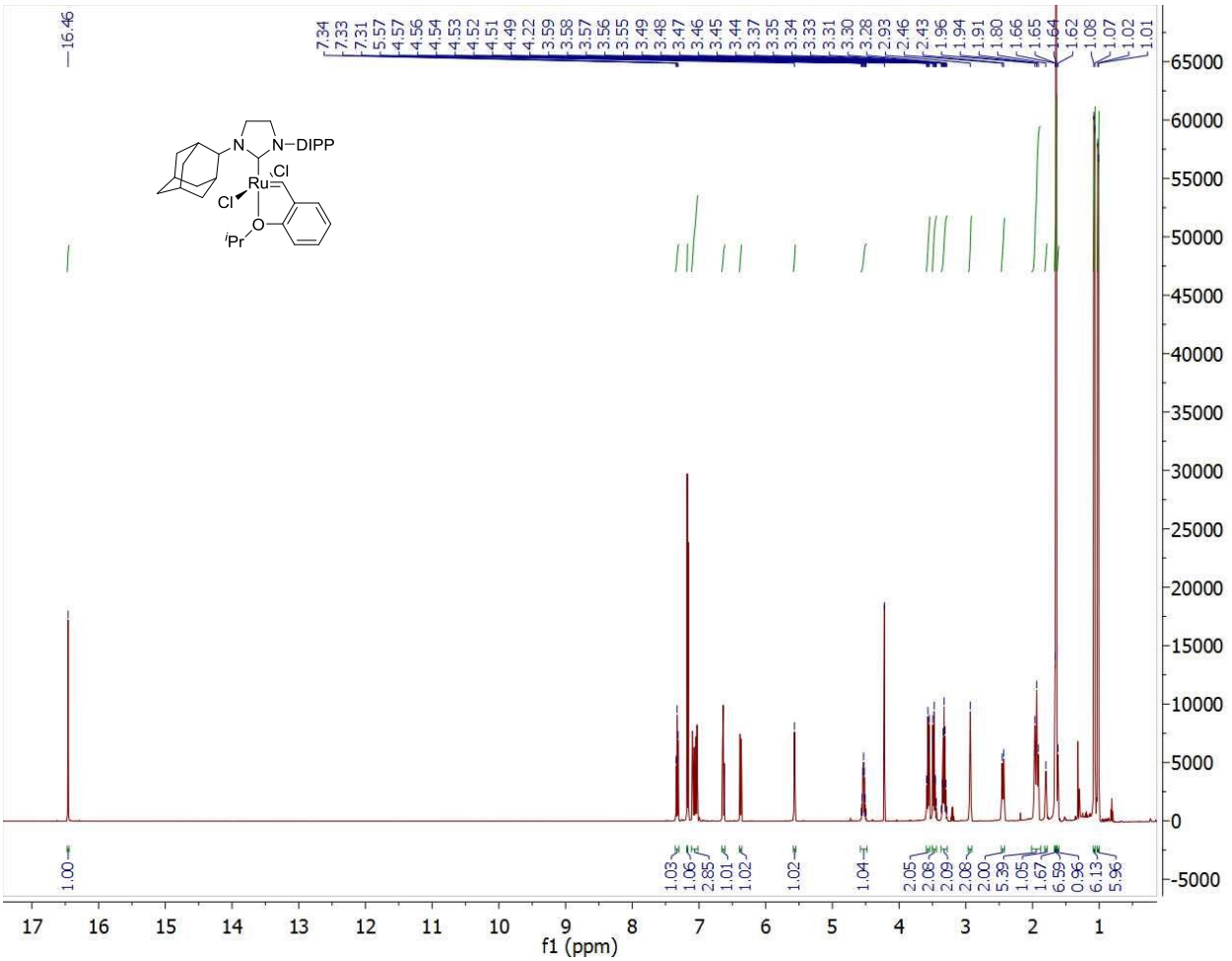

Figure S15. ^{1}H NMR (500 MHz) spectrum of **17** in C_6D_6.

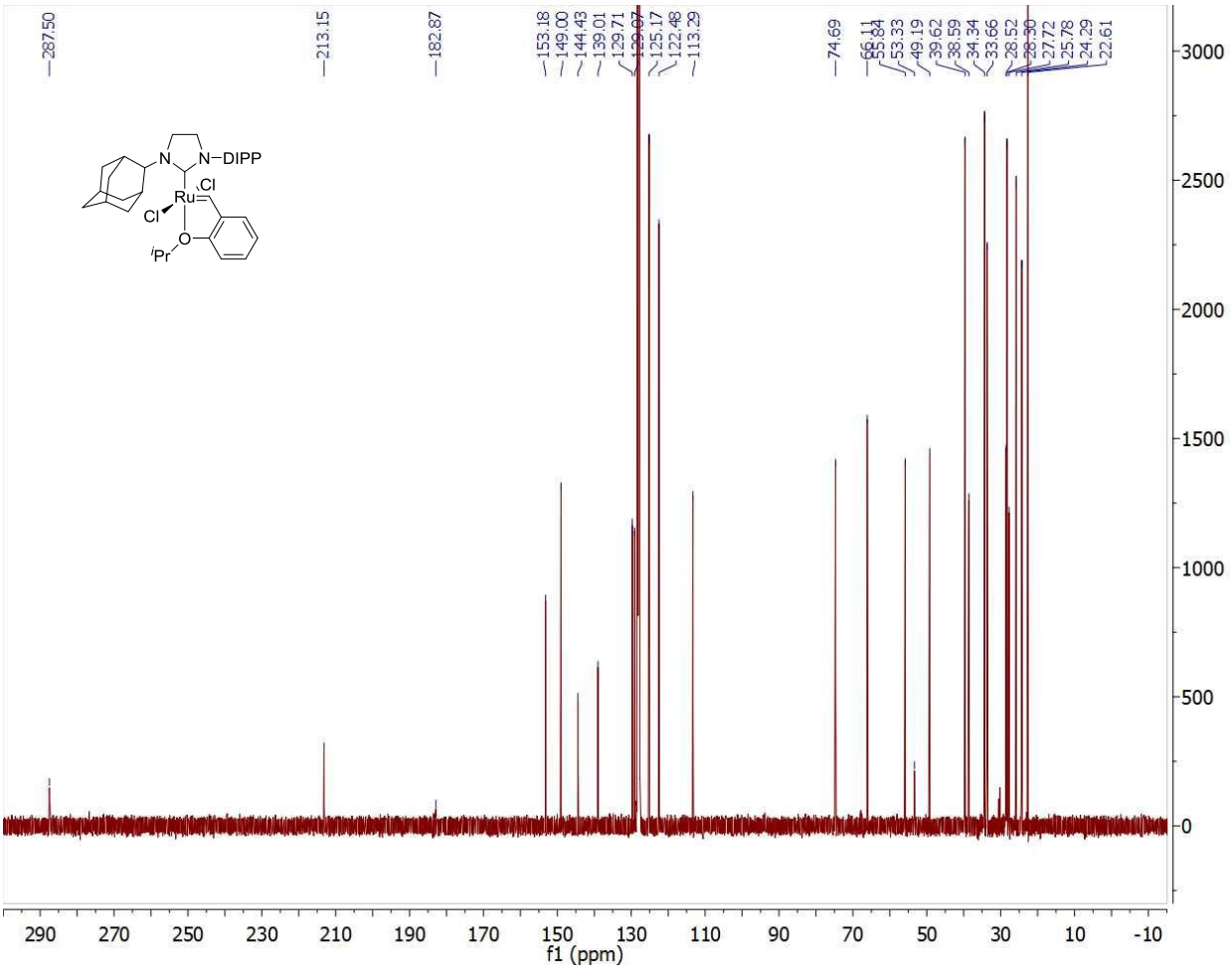

Figure S16. $^{13}C\{^{1}H\}$ NMR (126 MHz) spectrum of **17** in C_6D_6.

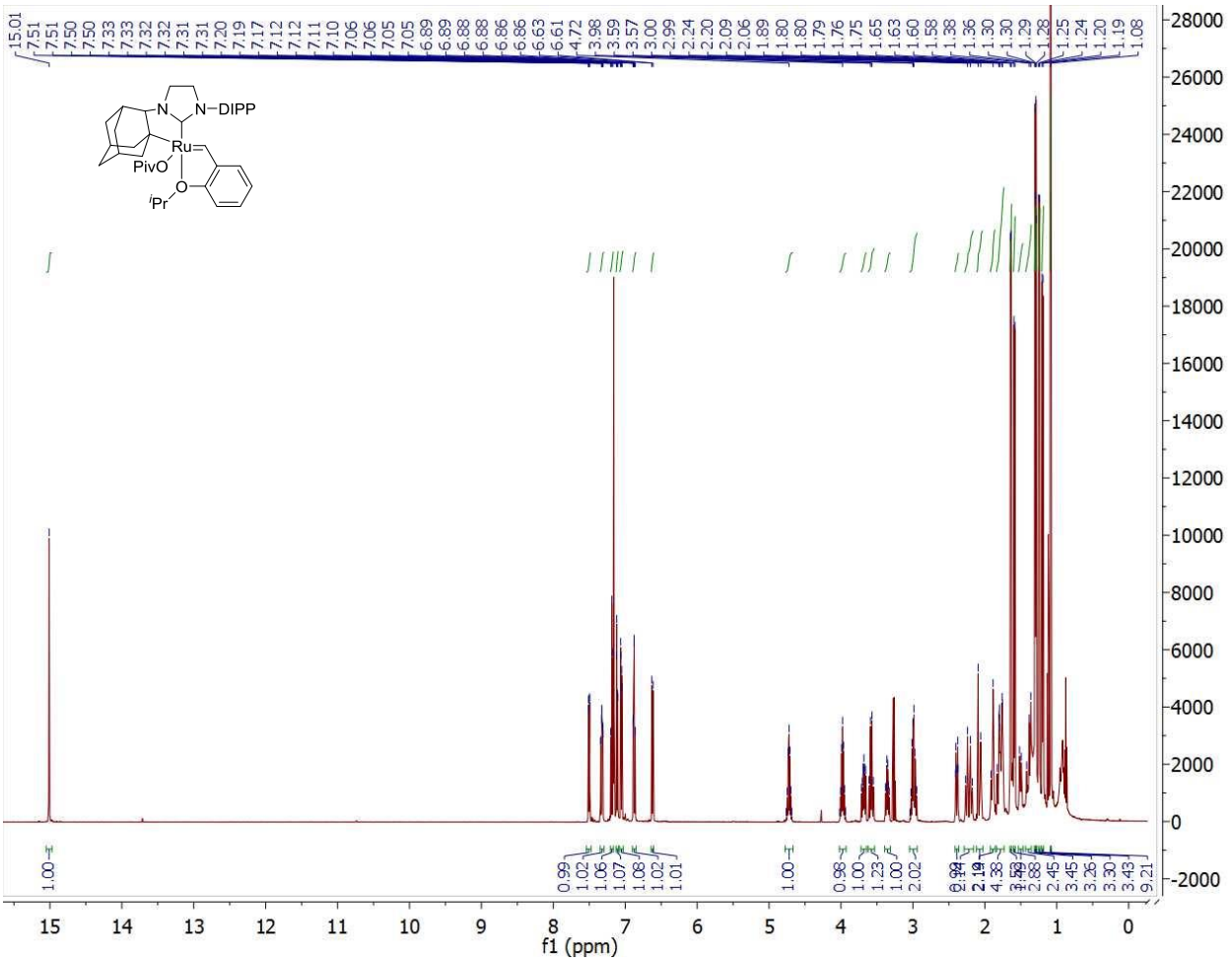

Figure S17. ^{1}H NMR (500 MHz) spectrum of **18** in C_6D_6.

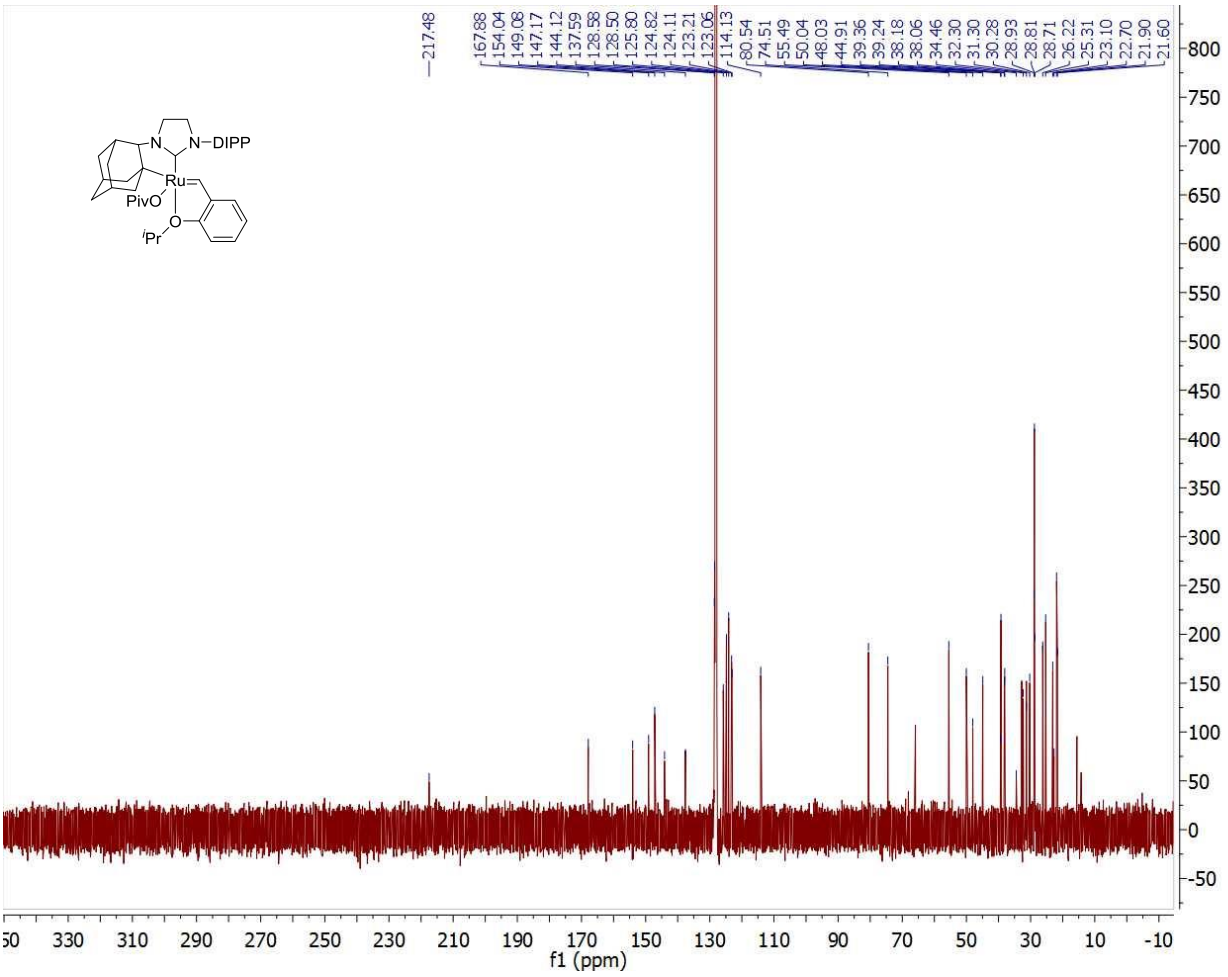

Figure S18. $^{13}C\{^{1}H\}$ NMR (126 MHz) spectrum of **18** in C_6D_6.

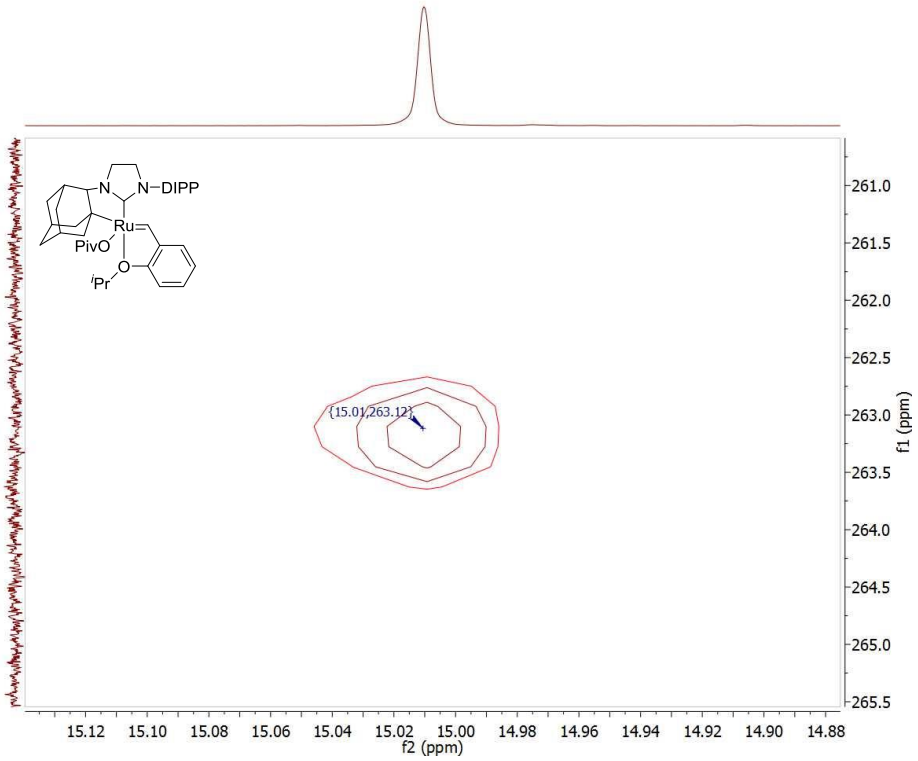

Figure S19. ^{1}H-^{13}C Coupled gHSQC spectrum of **18** in C_6D_6.

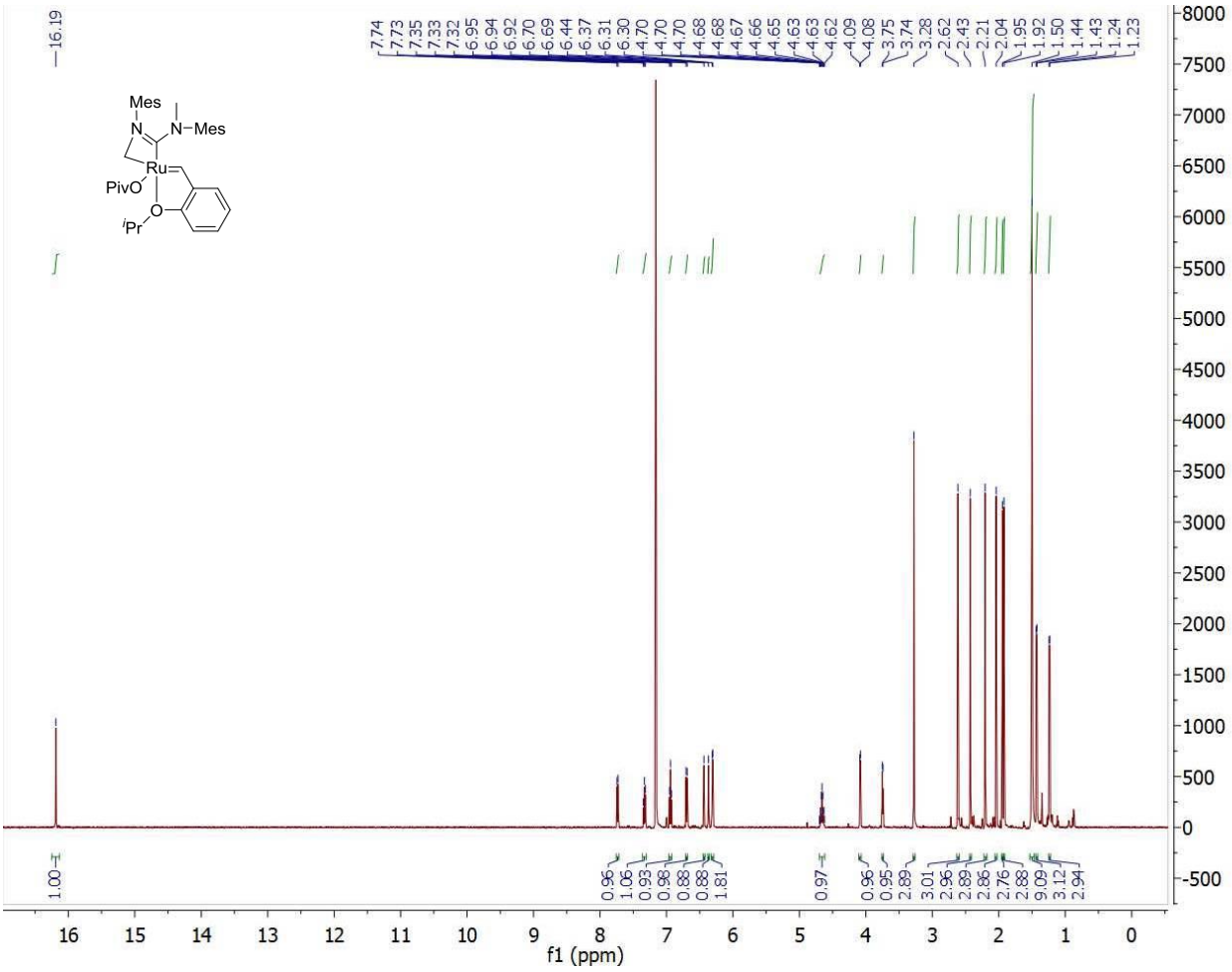

Figure S20. ^{1}H NMR (500 MHz) spectrum of **20** in C_6D_6.

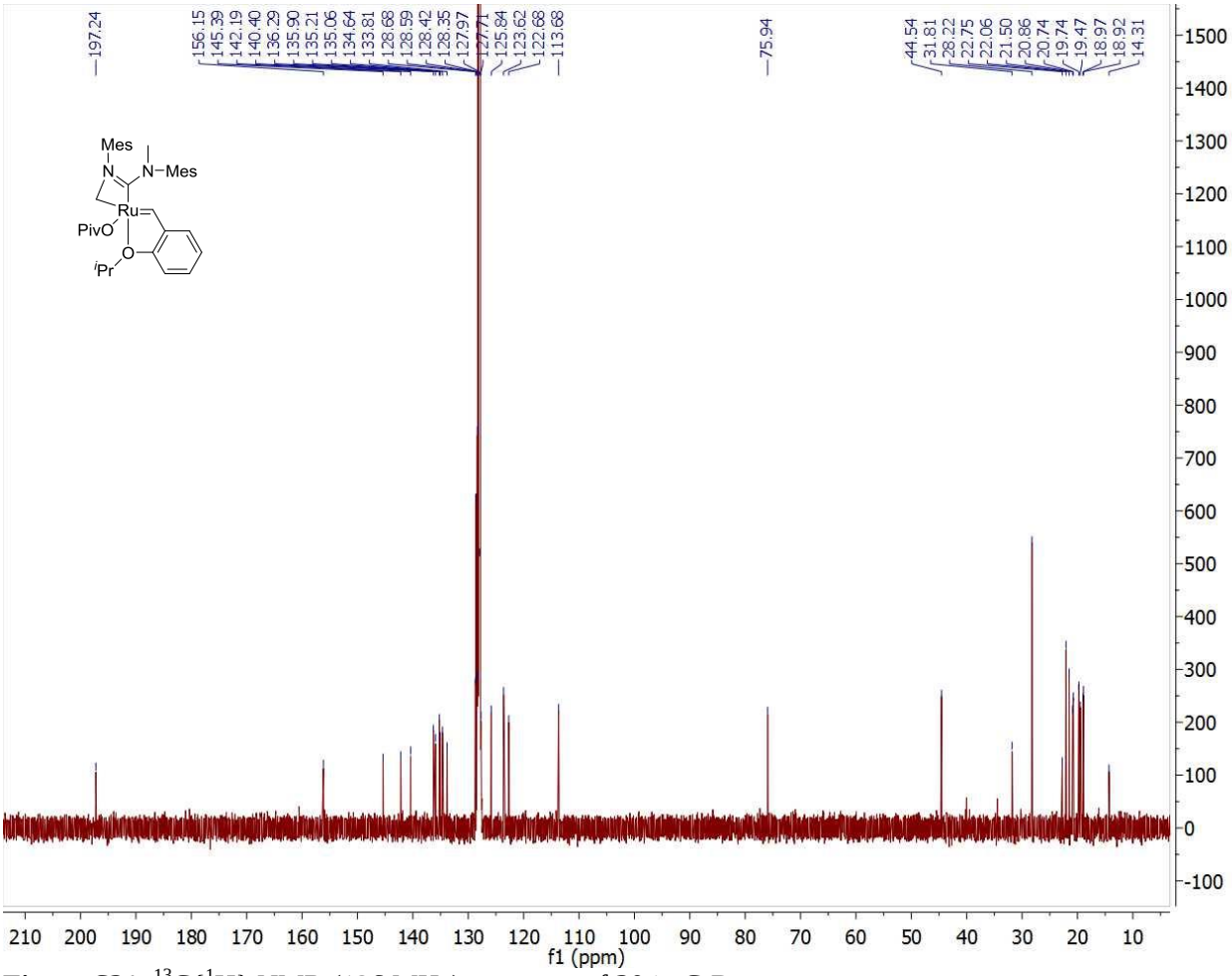

Figure S21. $^{13}C\{^{1}H\}$ NMR (126 MHz) spectrum of **20** in C_6D_6.

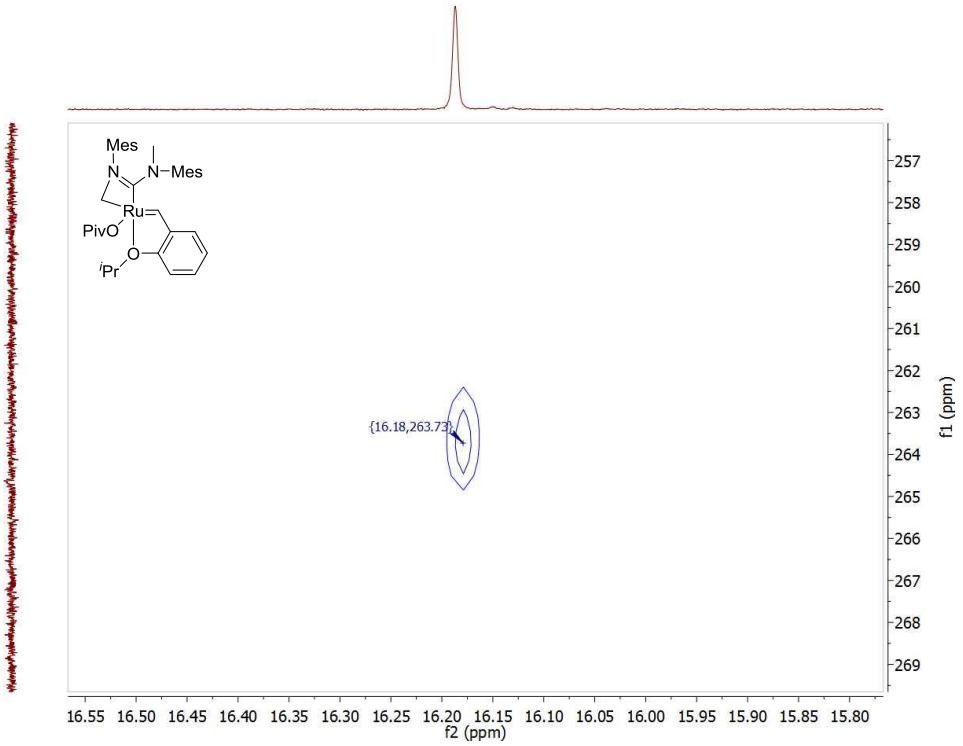

Figure S22. ^{1}H-^{13}C Coupled gHSQC spectrum of **20** in C_6D_6.

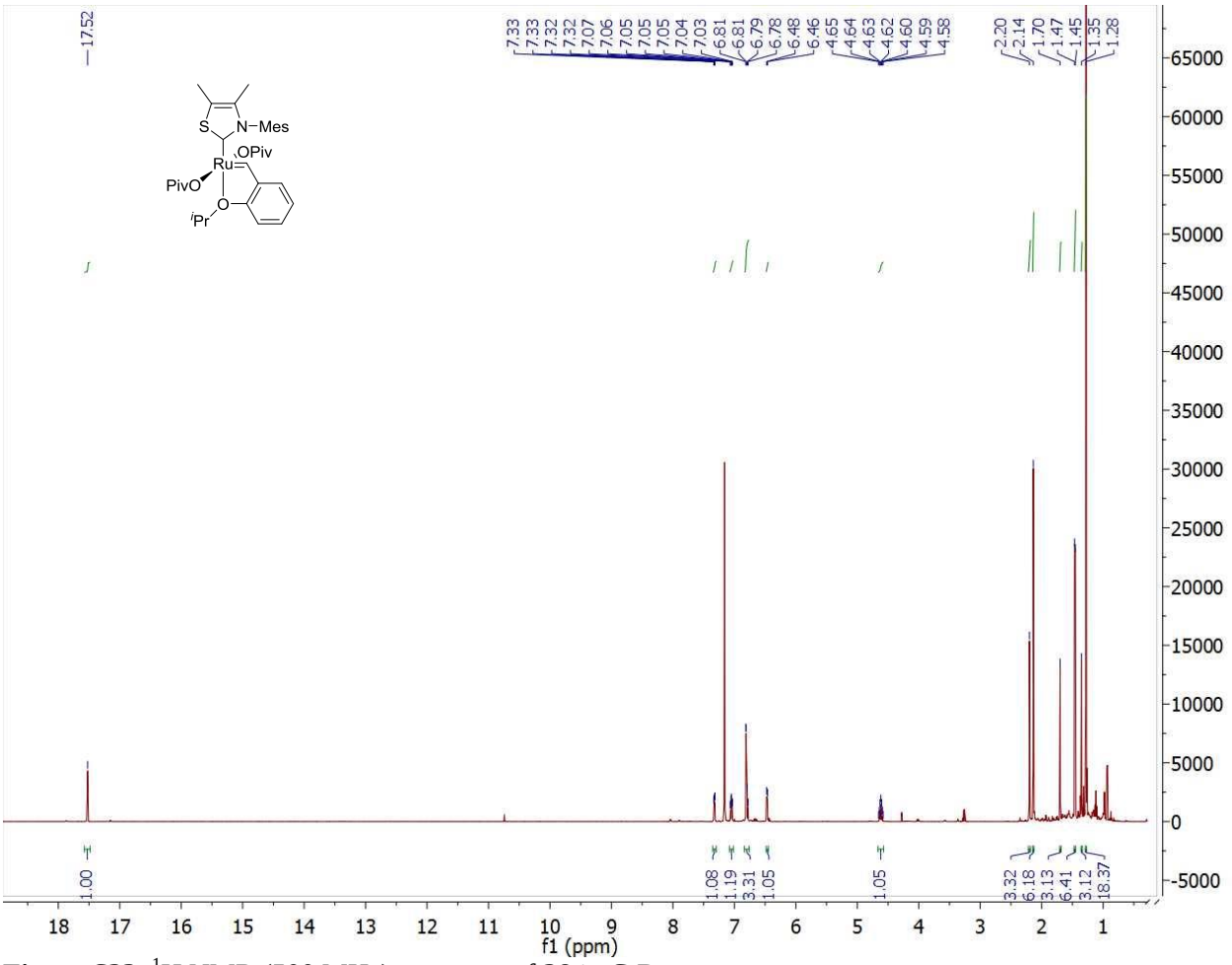

Figure S23. ^{1}H NMR (500 MHz) spectrum of **28** in C_6D_6.

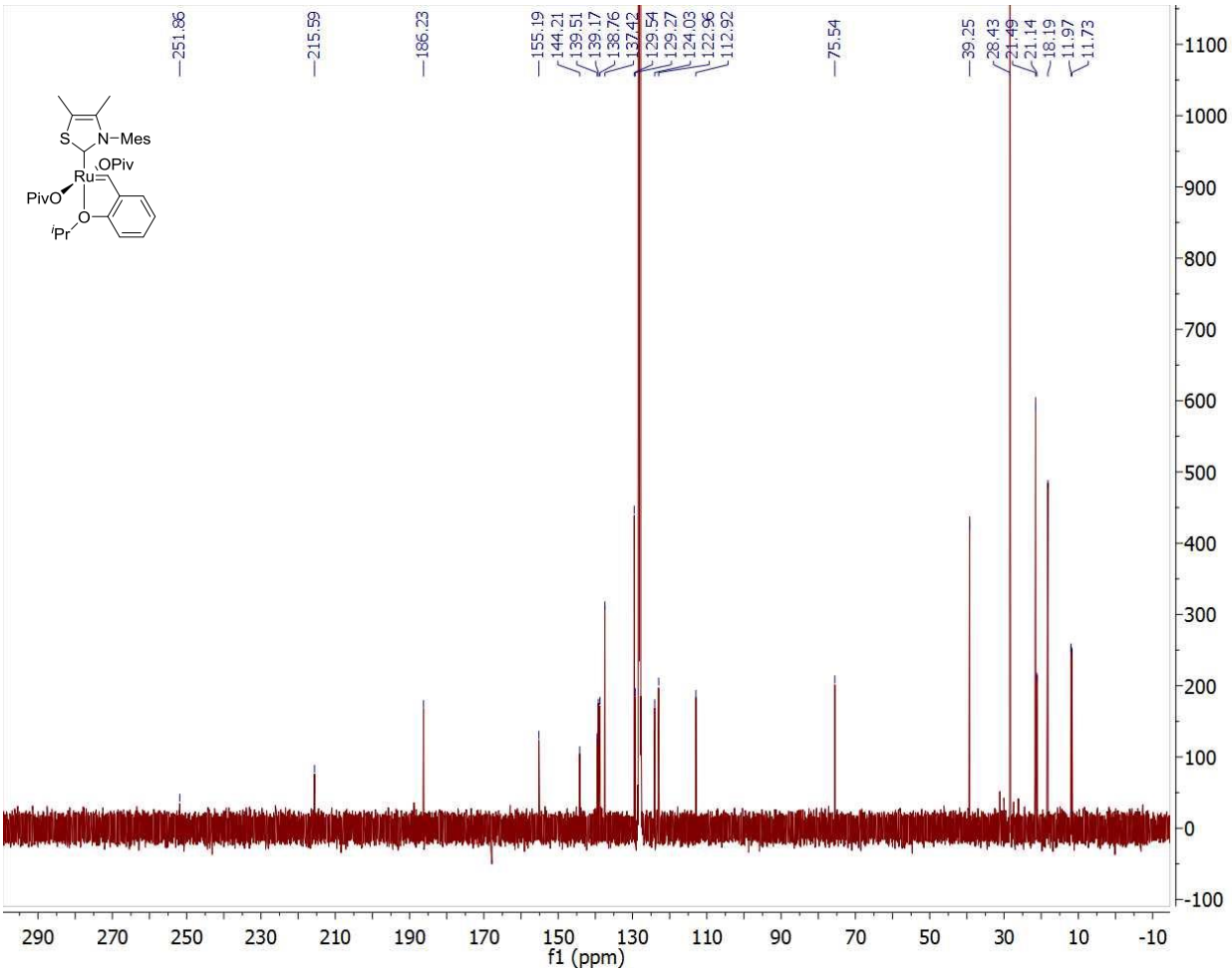

Figure S24. $^{13}C\{^{1}H\}$ NMR (126 MHz) spectrum of **28** in C_6D_6.

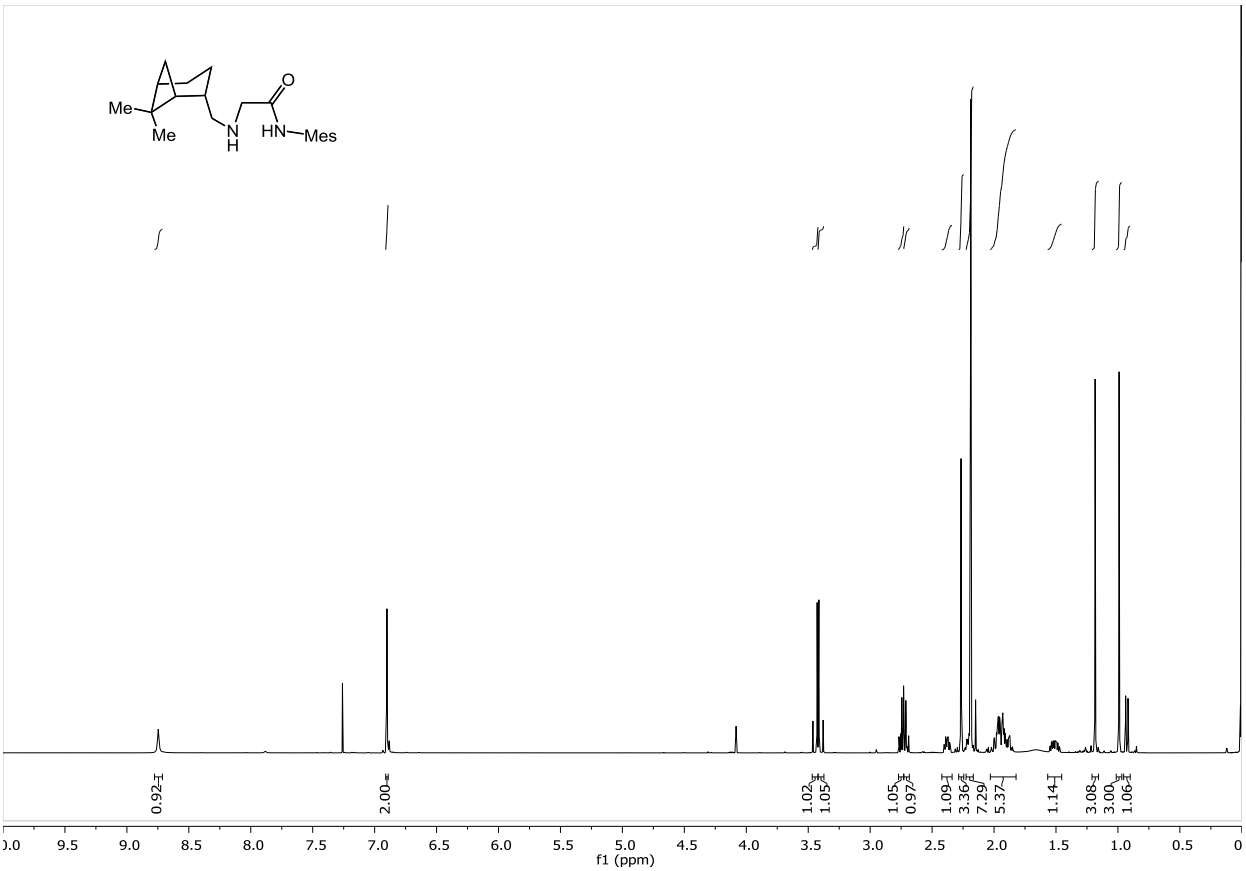

Figure S25. ^{1}H NMR (500 MHz) spectrum of **S3** in $CDCl_3$.

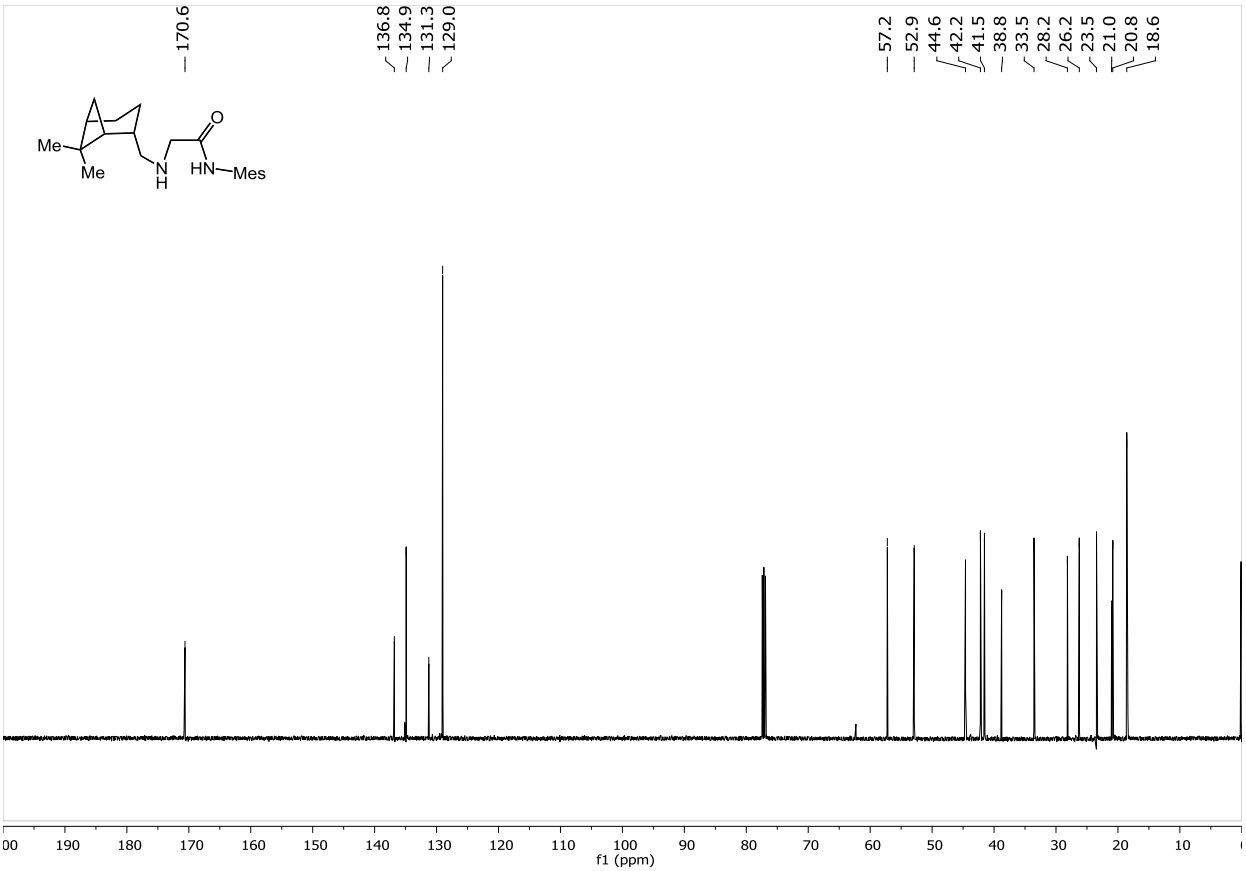

Figure S26. $^{13}C\{^{1}H\}$ NMR (126 MHz) spectrum of **S3** in $CDCl_3$.

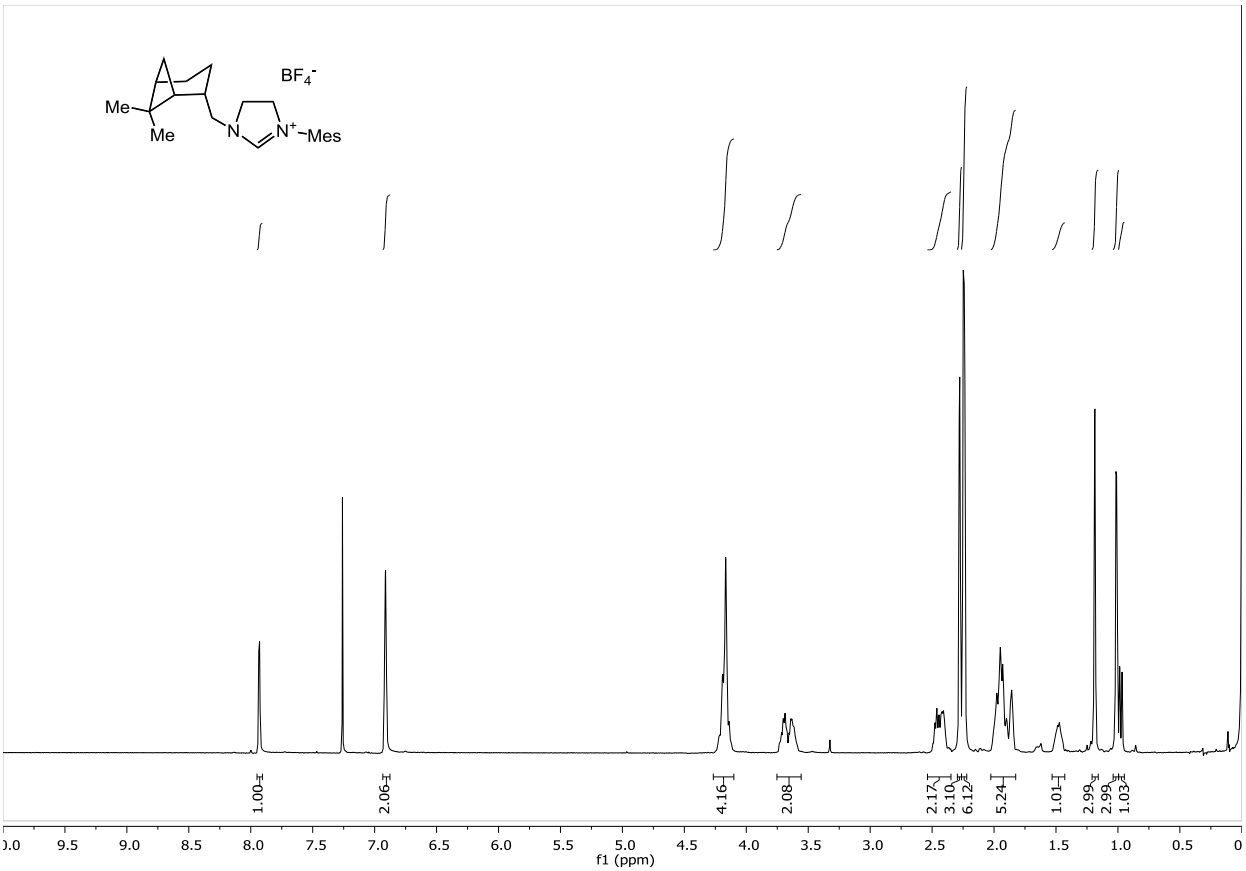

Figure S27. ^{1}H NMR (500 MHz) spectrum of **S4** in $CDCl_3$.

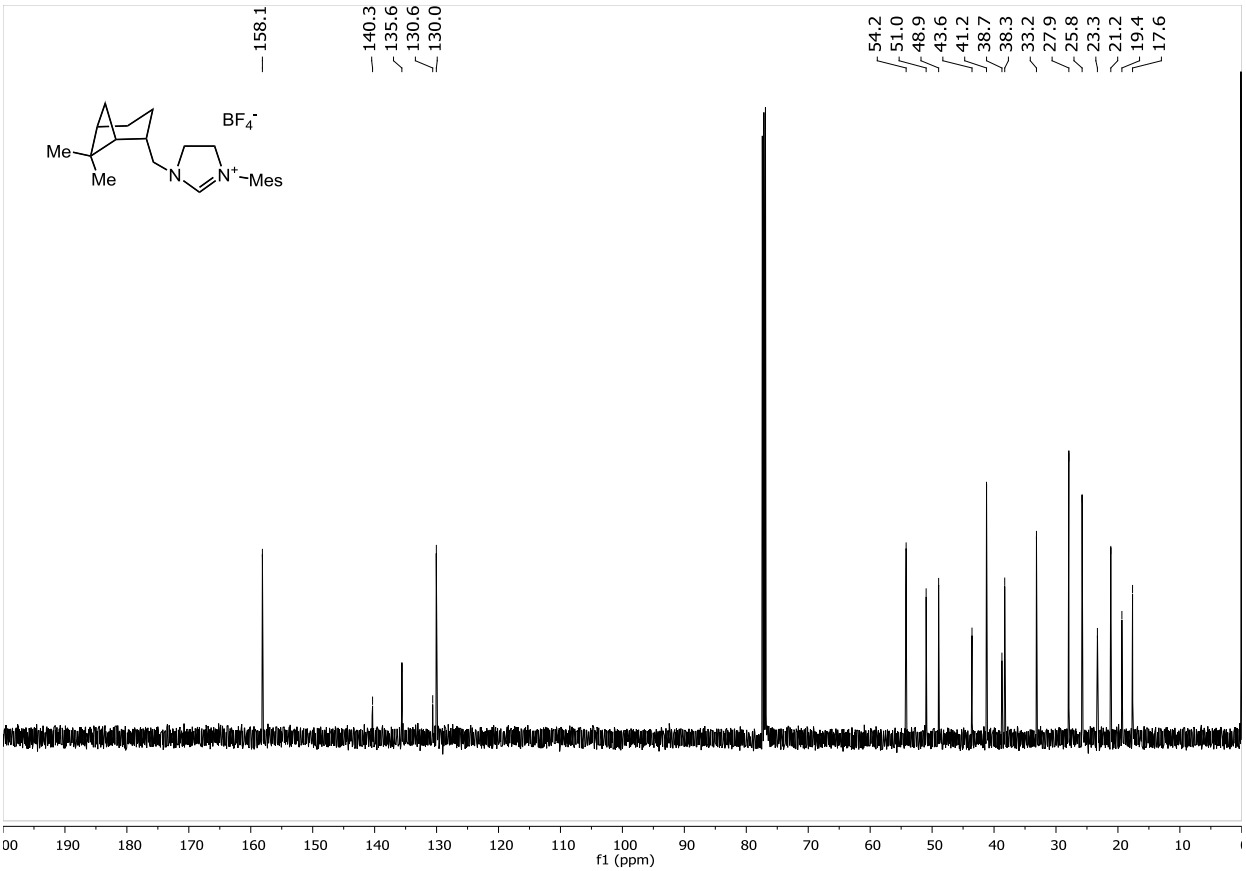

Figure S28. $^{13}C\{^{1}H\}$ NMR (126 MHz) spectrum of **S4** in $CDCl_3$.

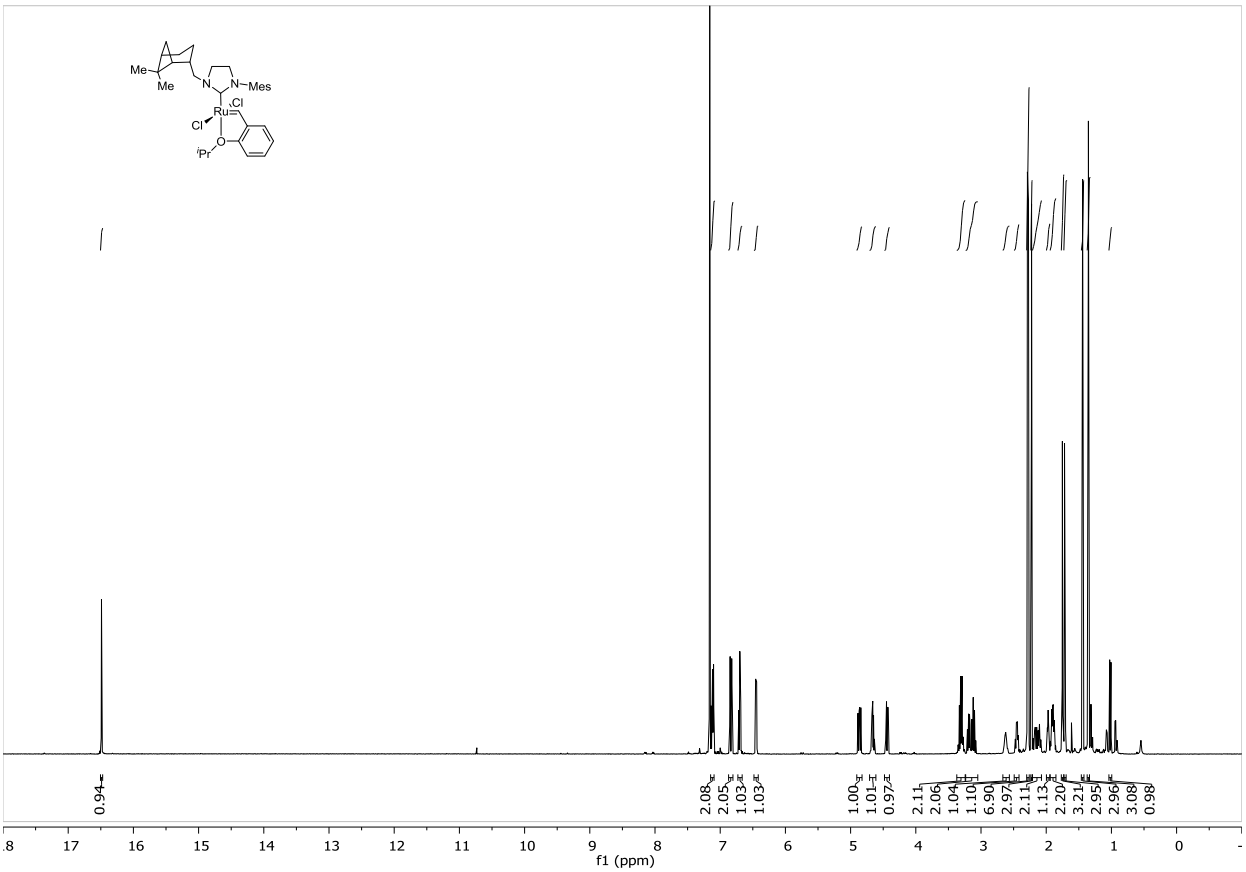

Figure S29. ^{1}H NMR (500 MHz) spectrum of **29** in C_6D_6.

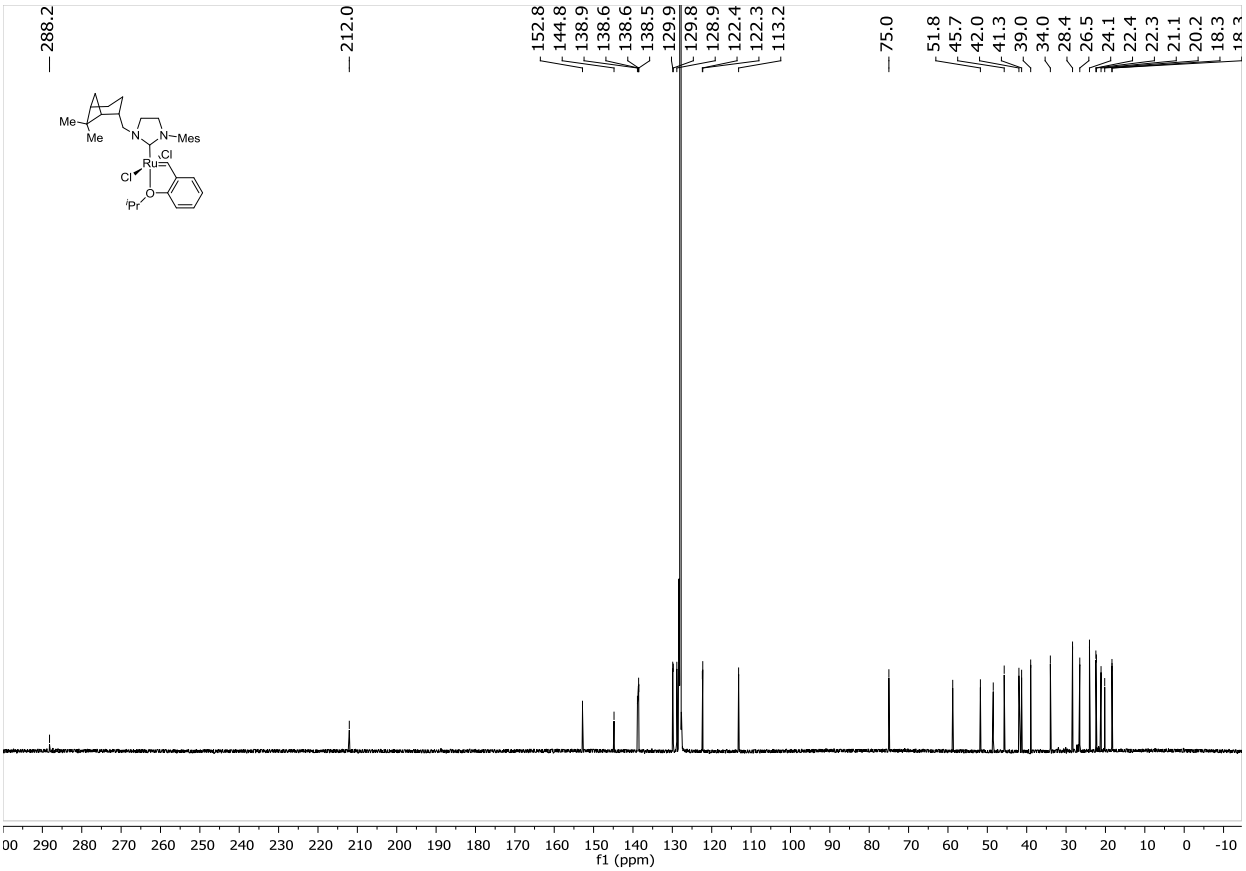

Figure S30. $^{13}C\{^{1}H\}$ NMR (126 MHz) spectrum of **29** in C_6D_6.

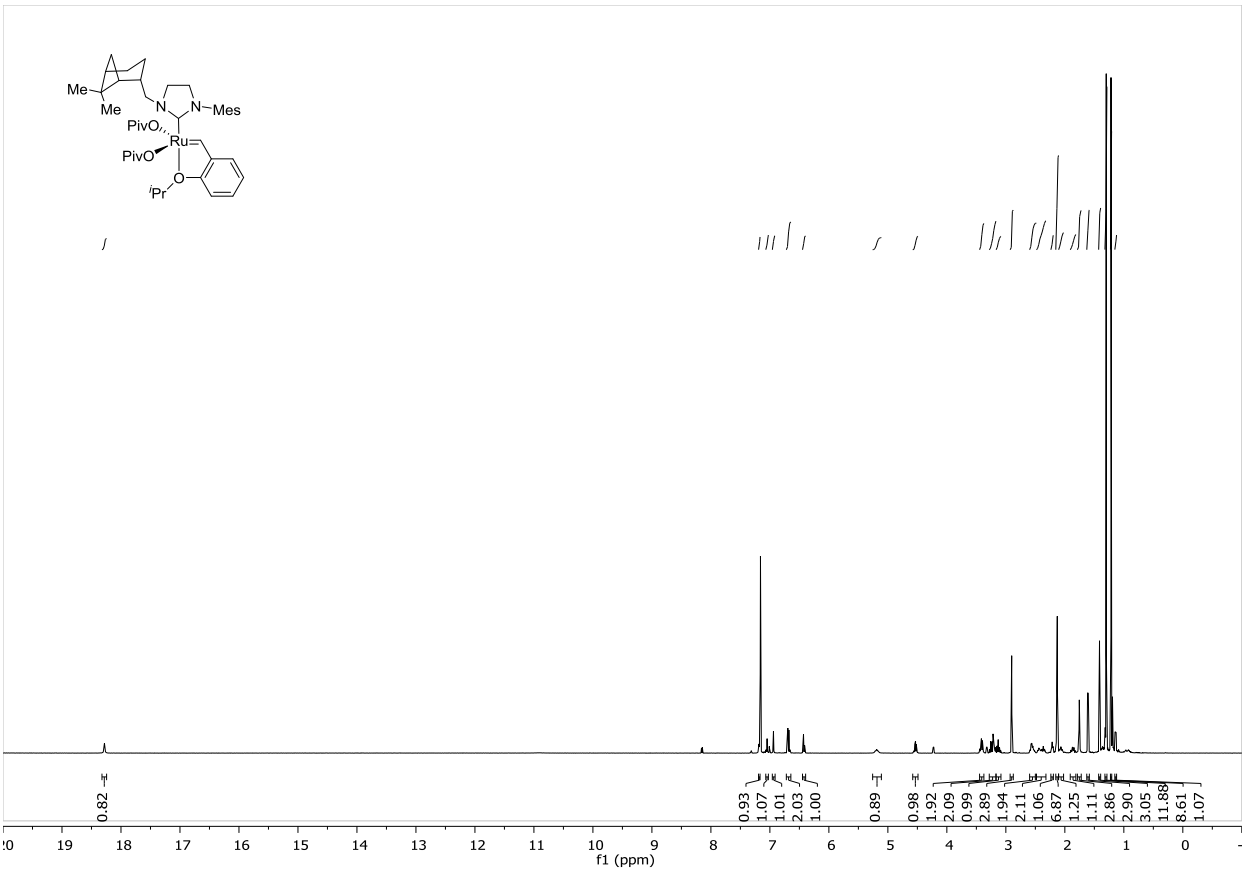

Figure S31. ^{1}H NMR (500 MHz) spectrum of **30** in C_6D_6.

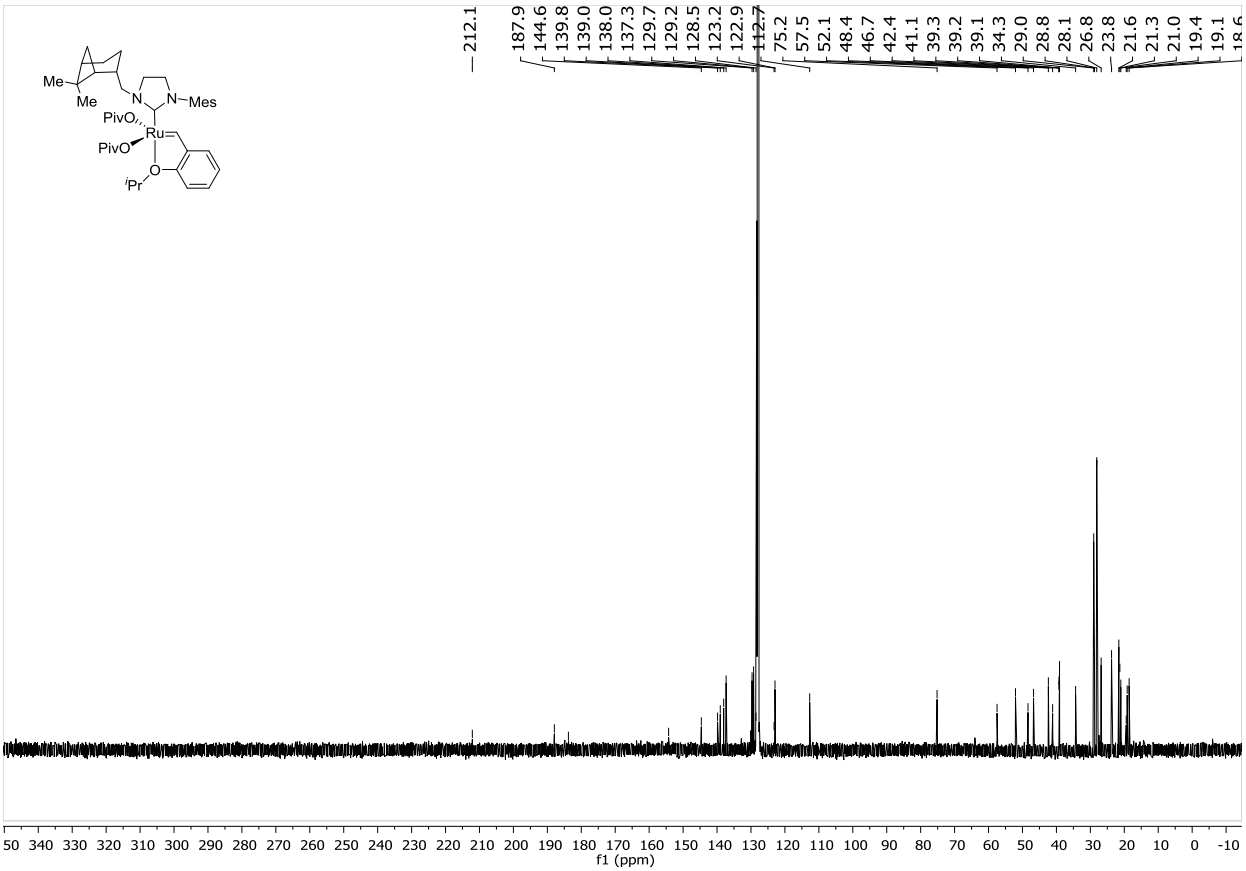

Figure S32. $^{13}C\{^{1}H\}$ NMR (126 MHz) spectrum of **30** in C_6D_6.

Comparison of 6-31G(d) and 6-31G(d,p) basis sets for hydrogen atoms in geometry optimizations

The B3LYP functional and the popular 6-31G(d) basis set were used in the geometry optimizations in this study ("method 1", LANL2DZ was used for Ru). To evaluate whether using polarization basis functions for hydrogen atoms is necessary in geometry optimizations, we performed test calculations for the reaction of complex **12** using B3LYP and the 6-31G(d,p) basis set in the geometry optimizations ("method 2", LANL2DZ for Ru). Single point calculations were performed at the same level of theory (M06/6-311+G(d,p)-SDD(Ru), with the SMD solvation model in THF). The computed activation energies and reaction energies using both levels of theories are summarized below. The two different levels of theories provide almost identical activation energies and reaction energies in the test calculations.

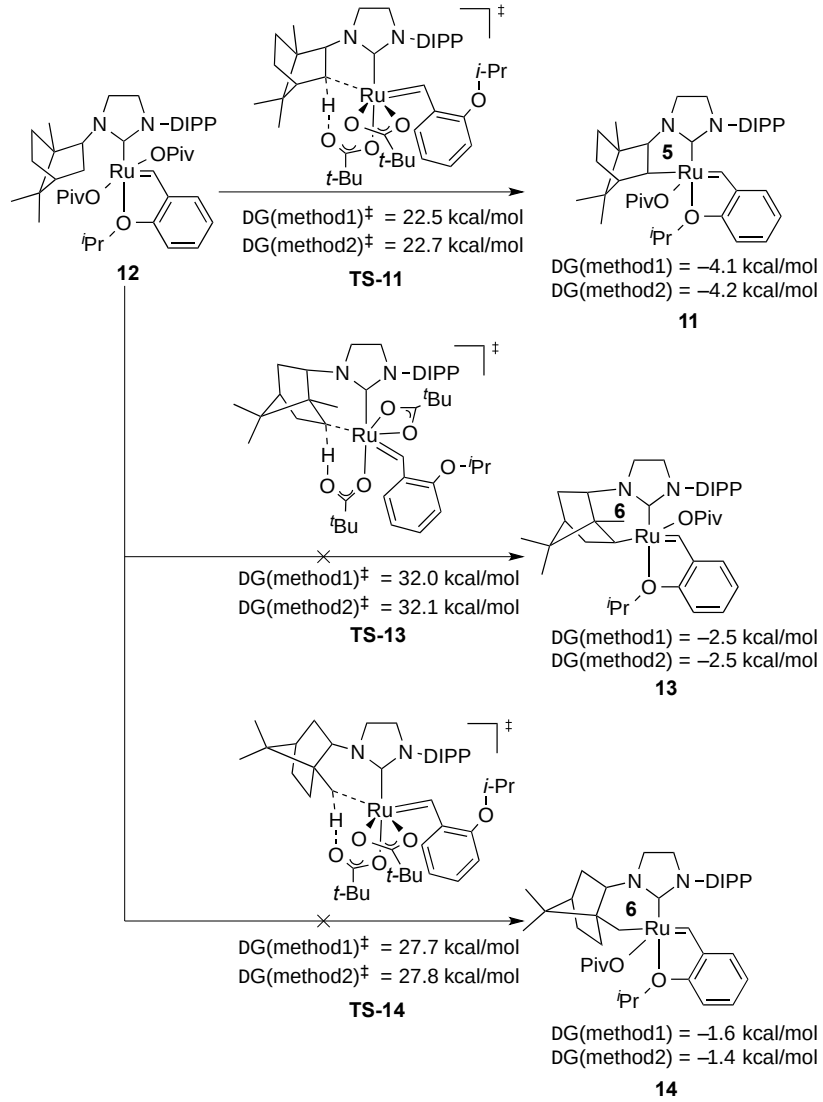

method1: M06/6-311+G(d,p)-SDD(Ru)/SMD(THF)//B3LYP/6-31G(d)-LANL2DZ(Ru)
method2: M06/6-311+G(d,p)-SDD(Ru)/SMD(THF)//B3LYP/6-31G(d,p)-LANL2DZ(Ru)

Conformers of TS-20 and 20

Two isomers for **TS-20** and the cyclometalated complex **20** were located. The conformer observed in the X-ray structure of the cyclometalated complex (**20**), in which the two mesityl groups are adjacent to each other, is predicted to be 0.9 kcal/mol more stable. The C-H activation transition states leading to the two conformers have very close activation barriers.

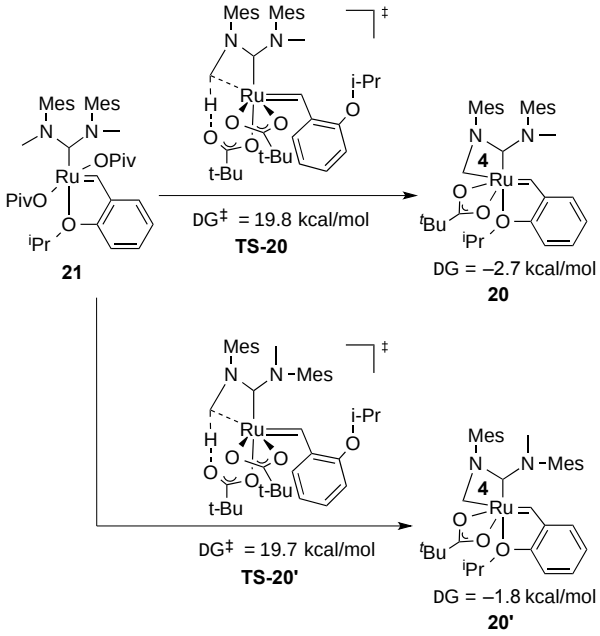

Optimized geometries of the C-H activation transition states to form the cyclometalated complexes 16, 18, and 31.

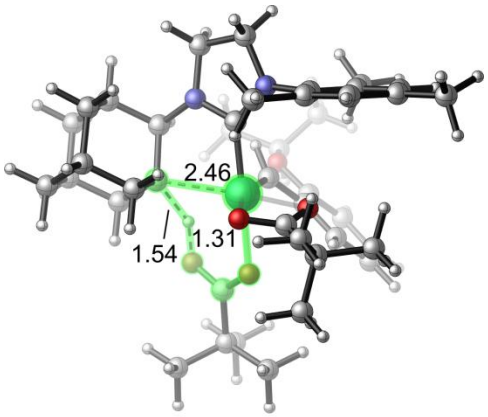

$\Delta G^{\ddagger}$ = 28.8 kcal/mol
TS-16

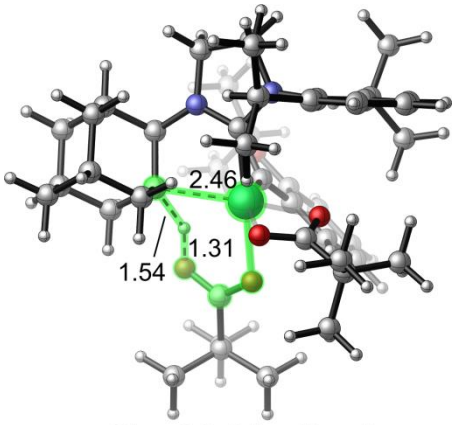

$\Delta G^{\ddagger}$ = 28.2 kcal/mol
TS-18

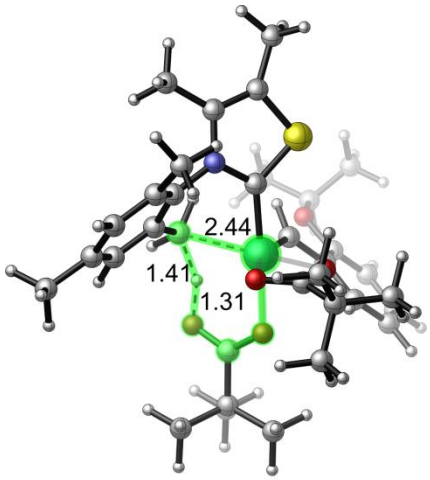

$\Delta G^{\ddagger}$ = 35.4 kcal/mol
TS-31

SCF energies, enthalpies at 298K, and Gibbs free energies at 298K for the optimized structures.

complex	E(B3LYP) (a.u.)	H(B3LYP) (a.u.)	G(B3LYP) (a.u.)	E(M06) (a.u.)	H(M06) (a.u.)	G(M06) (a.u.)	imaginary frequency (cm^{-1})
11	-1988.25815	-1987.296008	-1987.427026	-1988.432532	-1987.470391	-1987.601409	
12	-2335.30295	-2334.18093	-2334.332764	-2335.366182	-2334.244162	-2334.395996	
13	-1988.25418	-1987.291689	-1987.420199	-1988.432842	-1987.470351	-1987.598861	
14	-1988.253865	-1987.291524	-1987.423867	-1988.427364	-1987.465022	-1987.597365	
15-OPiv2	-2216.204565	-2215.193133	-2215.335496	-2216.319604	-2215.308172	-2215.450535	
16	-1869.153068	-1868.301603	-1868.420516	-1869.38693	-1868.535464	-1868.654377	
17-OPiv2	-2334.128144	-2333.026574	-2333.173852	-2334.190165	-2333.088595	-2333.235873	
18	-1987.079818	-1986.137904	-1986.261896	-1987.255378	-1986.313464	-1986.437456	
20	-1829.821074	-1829.005904	-1829.136602	-1830.054711	-1829.23954	-1829.370238	
21	-2176.863586	-2175.888204	-2176.036776	-2176.993957	-2176.018575	-2176.167147	
22	-1829.815819	-1828.99959	-1829.127015	-1830.054711	-1829.238481	-1829.365906	
28	-2246.953231	-2246.154959	-2246.288188	-2247.229484	-2246.431212	-2246.564441	
31	-1899.894008	-1899.254982	-1899.366133	-1900.280931	-1899.641905	-1899.753056	
TS-11	-2335.253773	-2334.138228	-2334.291618	-2335.322373	-2334.206828	-2334.360218	-1342.3
TS-13	-2335.234333	-2334.119021	-2334.269804	-2335.309565	-2334.194253	-2334.345036	-1444.4
TS-14	-2335.249591	-2334.133865	-2334.286588	-2335.314862	-2334.199136	-2334.351859	-1374.3
TS-16	-2216.143881	-2215.139436	-2215.281312	-2216.267234	-2215.26279	-2215.404666	-1488.5
TS-18	-2334.070761	-2332.975957	-2333.123282	-2334.138365	-2333.043561	-2333.190886	-1484.5
TS-20	-2176.823418	-2175.85512	-2176.010736	-2176.94828	-2175.979982	-2176.135598	-1239.3
TS-22	-2176.814576	-2175.845209	-2175.995799	-2176.943285	-2175.973918	-2176.124508	-1386.4
TS-31	-2246.89135	-2246.099086	-2246.234015	-2247.166874	-2246.37461	-2246.509539	-1386.5
PivOH	-347.017538	-346.860885	-346.902513	-346.916158	-346.759505	-346.801133	

Cartesian coordinates of all optimized structures are provided in ".xyz" file format in the Supporting Information.

[1] Bessel, M.; Rominger, F.; Straub, B. F. *Synthesis* **2010**, *9*, 1459